HHS Public Access

Author manuscript

J Med Chem. Author manuscript; available in PMC 2022 July 24.

Published in final edited form as:

J Med Chem. 2021 May 27; 64(10): 6608–6620. doi:10.1021/acs.jmedchem.0c01926.

Gold(I) phosphine derivatives with improved selectivity as topically active drug leads to overcome 5-nitroheterocyclic drug resistance in *Trichomonas vaginalis*

Yukiko Miyamoto[†], **Shubhangi Aggarwal**[‡], **Jeff Joseph A. Celaje**[‡], **Sozaburo Ihara**[†], **Jonathan Ang**[†], **Dmitry B. Eremin**[‡], **Kirkwood M. Land**[§], **Lisa A. Wrischnik**[§], **Liangfang Zhang**[‖], **Valery V. Fokin**[‡], **Lars Eckmann**[*,†]

[†]Department of Medicine, University of California, San Diego, La Jolla, California 92093, U.S.A.

[‡]Department of Chemistry, Dornsife College of Letters, Arts and Sciences, University of Southern California, Los Angeles, California 90089, U.S.A.

[§]Department of Biological Sciences, University of the Pacific, Stockton, California 95211, U.S.A.

[‖]Department of NanoEngineering, University of California, San Diego, La Jolla, California 92093, U.S.A.

Abstract

Trichomonas vaginalis causes the most common, non-viral sexually-transmitted infection. Only metronidazole (Mz) and tinidazole are approved for treating trichomoniasis, yet resistance is a clinical problem. The gold(I) complex, auranofin, is active against *T. vaginalis* and other protozoa, but has significant human toxicity. In a systematic structure-activity exploration, we show here that diversification of gold(I) complexes, particularly as halides with simple C1-C3 trialkyl phosphines or as bistrialkyl phosphine complexes , can markedly improve potency against *T. vaginalis* and selectivity over human cells compared to the existing anti-rheumatic gold(I) drugs. All gold(I) complexes inhibited the two most abundant isoforms of the presumed target enzyme, thioredoxin reductase, but a subset of compounds were markedly more active against live *T. vaginalis* than the enzyme, suggesting that alternative targets exist. Furthermore, all tested gold(I) complexes acted independently of Mz and were able to overcome Mz resistance, making them candidates for the treatment of Mz-refractory trichomoniasis.

Graphical Abstract

[*]Corresponding author: Lars Eckmann, Department of Medicine, 9500 Gilman Drive, La Jolla, CA 92093-0623, Phone (858) 534-0683, leckmann@ucsd.edu.

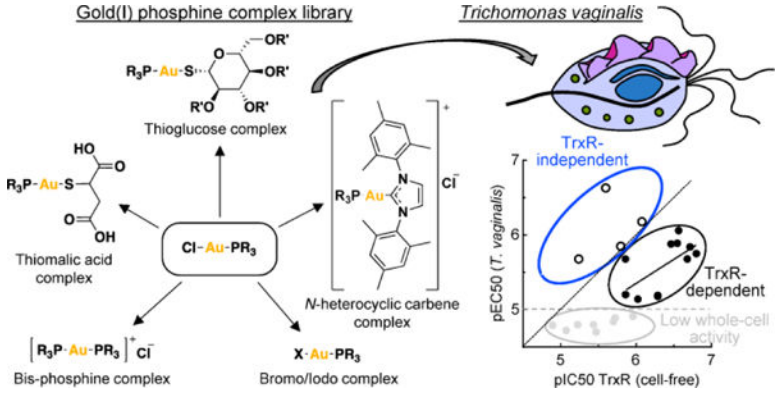

INTRODUCTION

The protozoan parasite, *Trichomonas vaginalis*, is the causative agent of the most common, non-viral sexually-transmitted infection, with 5–7 million cases in the United States and >200 million in the world each year.[1] Symptomatic infection in women is characterized by vaginal discharge, dysuria, and abdominal pain. Infected men typically have few symptoms, but urethritis, prostatitis, balanoposthitis, and epididymitis can occur. Trichomoniasis increases the risk of adverse pregnancy outcomes and HIV transmission, and the incidence and severity of cervical and prostate cancers.[2, 3] Infection can persist in women for months or even years compared to generally less than ten days in men, making treatment of trichomoniasis particularly urgent in women.[4]

Only two drugs are FDA-approved for the treatment of trichomoniasis, the nitro-heterocyclic compounds metronidazole (Mz) and tinidazole.[5] Oral drug administration leads to clinical and microbiological cure in the majority of cases, but treatment failures occur in a significant fraction of patients. Surveillance studies have found Mz resistance in 2.4–9.6% of isolates in the United States, 2.2% in Spain, and 17.4% in Papua New Guinea.[6, 7] Mz and other nitro-heterocyclic drugs are prodrugs that must be reduced to reactive intermediates by microbial reductases before they forms adducts that inactivate different cellular targets.[8] Consequently, Mz resistance is mediated by diminished expression or function of major drug-reducing pathways, including pyruvate:ferredoxin oxidoreductase and ferredoxin [9–11], thioredoxin reductase (TrxR) [12], flavin reductase, and alcohol dehydrogenase.[13–15] These redox pathways normally allow the parasite to cope with oxidative stresses encountered under microaerophilic growth conditions in the host. In particular, thioredoxin-dependent peroxidases constitute a central antioxidant defense in *T. vaginalis*, which lack the defenses of glutathione reductase and catalase found in mammalian cells.[16]

In efforts to discover new agents against trichomoniasis, numerous compounds have been tested *in vitro* against *T. vaginalis*. For example, a screen of 1,040 compounds in the U.S. Drug Collection Library revealed several drugs with significant trichomonacidal activity.[17] None of these drugs were as effective as nitro antimicrobials and none were tested in animal models or humans. Other drugs targets such as carbonic anhydrases show significant structural differences between *T. vaginalis* and human cells that may be exploited for new drug development, although strong candidate drugs have not yet been

identified.[18, 19] We discovered recently that the anti-rheumatic gold drug, auranofin (AF), is active against trichomonads in the low μM range and efficacious in a vaginal infection model.[20] AF also has activity against other protozoa, including *Entamoeba histolytica*, *Giardia lamblia*, and *Plasmodium*[21, 22] First approved in 1985, AF is the only orally active gold compound with significant therapeutic efficacy against rheumatoid arthritis. Two other gold compounds, gold sodium thiomalate and gold thioglucose, have been approved as injectable drugs for rheumatoid arthritis, but all three compounds have significant adverse effects, including most prominently gastrointestinal complaints, and their use has declined over the years.[23] The mechanisms of the anti-inflammatory or anti-microbial actions of AF are not completely understood, but the drug is a potent inhibitor of TrxR and concurrently, compromises the ability of *T. vaginalis* and other protozoa to survive oxidative stress.[20, 21, 24, 25]

Given the significant toxicity of FDA-approved gold compounds, attempts have been made to find gold derivatives with better activity profiles. For example, gold(I) *N*-heterocyclic carbene (NHC) complexes have excellent activity and selectivity against the protozoan parasites, *Leischmania*[26], *Toxoplasma gondii*[27], and *Trypanosoma brucei*.[28] Similarly, analogues of AF have improved activity, compared to AF, against a range of bacterial targets, including *Enterococcus faecium*, *Staphylococcus aureus*, *Klebsiella pneumoniae*, *Acinetobacter baumannii*, *Pseudomonas aeruginosa*, and *Enterobacter* spp.[29] Encouraged by these findings, we undertook a systematic exploration of gold(I) derivatives as agents against *T. vaginalis* with the goal to identify compounds with markedly improved selectivity compared to AF and the ability to overcome Mz resistance.

RESULTS

Organic thiol ligands in gold(I) complexes compromise selectivity for *T. vaginalis* over human cells

To explore the structure-activity landscape of gold(I) complexes against *T. vaginalis*, we acquired and synthesized a range of complexes with different organic and inorganic ligands, using the general synthetic schemes outlined in Fig. 1.

We had previously discovered that AF is active against *T. vaginalis* in the low μM range.[20] However, testing for human cytotoxicity in HeLa cells revealed that it is slightly more toxic against human cells than the parasite, so its selectivity index is <1 (Fig. 2), questioning its viability as a therapeutic agent against trichomoniasis. To determine whether other FDA-approved gold(I) compounds might have a more favorable activity profile, we tested aurothioglucose (ATG) and sodium aurothiomalate (ATM). Both have been used as injectable anti-rheumatic agents, but their use has declined over the years due to significant adverse effects during long-term use.[23] Those two drugs barely showed activity against *T. vaginalis* (Fig. 2). These findings indicate that AF is a useful starting point for SAR exploration for gold(I) complexes, while ATG and ATM are not promising as trichomonacidal agents. Consequently, we systematically varied various side chains and ligands with the goal to improve potency of gold(I) complexes against *T. vaginalis* and selectivity over mammalian cells. These efforts purposefully focused on biological activity in live cells rather than inhibition of any particular targets, since the targets of gold(I)

compounds in the parasite are not well understood and can thus not serve as a direct guide to improving activity profiles.

Ligand swapping showed that addition of the triethyl phosphine ligand of AF to either ATG or AMG in compounds **1** and **2**, respectively, improved trichomonacidal activity similar to AF, but these compounds were also toxic in human cells and thus showed no improvement in selectivity over AF (Fig. 2). Replacement of the thiol ligand in AF with a substituted NHC (**3**), which was prevously shown to improve antimicrobial activity in other parasites [26, 28], did not enhance trichomonacidal activity, but strongly increased human cytotoxicity, leading to a ~10-fold reduction in selectivity compared to AF (Fig. 2). In contrast, loss of the organic thiol ligands of AF, ATG and ATM by replacement with a simple halide, chloride (**4**), markedly reduced human cytotoxicity but slightly increased activity against *T. vaginalis*, thereby improving selectivity by ~8-fold compared to AF (Fig. 2).

To determine if the negative influence of the thiol ligands of AF, ATG and ATM on selectivity might be affected by the nature of the phosphine ligand in the gold(I) complex, we replaced the triethyl phosphine ligand in the three FDA-approved gold(I) compounds with tributyl phosphine to yield compounds **5**, **6** and **7**, as well as in the NHC-substituted compound **3** to yield compound **8** (Fig. 2). Three of the four tributyl gold(I) compounds, **6**, **7** and **8**, had similar trichomonacidal activity and selectivity as their triethyl partners, while the fourth compound, **5**, had ~10-fold lower activity against both *T. vaginalis* and human cells with no improvement in selectivity (Fig. 2). Notably, complete removal of the organic thiol ligands from the tributyl phosphines and replacement with chloride in compound **9** abolished all activity (Fig. 2). We conclude from these experiments that the organic thiol ligands have only modest effects on trichomonacidal activity but markedly compromise selectivity over human cells.

Phosphine ligands in gold(I) complex control trichomonacidal activity and selectivity

Given the negative effects of the various organic thiol ligands (Fig. 2), we abandoned further thiol explorations and instead focused on the importance of different phosphine ligands in thiol-free gold(I) complexes with a simple chloride ligand. A systematic series of linear and branched alkyl phosphines with increasing chain lengths showed that gold(I) compounds with trimethyl (**10**), triethyl (**4**), tripropyl (**11**) and triisopropyl (**12**) phosphines had excellent and similar trichomonacidal activity in the low μM range combined with decreased human cytotoxicity and corresponding increases in selectivity, while the tributyl (**9**) and triisobutyl (**17**) phosphine gold(I) complexes were inactive in both *T. vaginalis* and human cells (Fig. 3). Furthermore, bis-phosphine complexes with trimethyl (**13**), triethyl (**14**), tripropyl (**15**), or triisopropyl (**16**) phosphine were as or moderately more active against both *T. vaginalis* and human cells, but generally had similar selectivity compared to the corresponding monophosphine complexes (Fig. 3). Replacement of the linear alkyls with one, two or three phenyls in compounds **18**, **19** and **20** compromised selectivity or overall activity or both, as did substitutions of the phenyl rings in the *para* position with methyl in compound **21** or trifluoromethyl in **22** (Fig. 3). Together, these SAR explorations indicate that gold(I) complexes with simple trialkyls of C1-C3 chain length have the most promise

for compounds with excellent trichomonacidal activity and markedly improved selectivity over human cells compared to the three FDA-approved gold(I) drugs.

Influence of halide in gold(I) complex on activity and selectivity

Because replacement of the organic thiol group with chloride markedly improved compound selectivity, we explored whether other halides could lead to further improvements. For two of the most selective phosphine ligands, trimethyl (**10**) and triethyl (**4**), we synthesized compounds with bromide (**23**, **24**) or iodide (**25**, **26**) in the gold(I) complex rather than chloride. Complexes with bromide and iodide displayed 5- to 10-fold reduced trichomonacidal activity compared to the chloride counterparts (Fig. 4). Human cytotoxicity also decreased but either to a lesser extent or to below the assay sensitivity. Thus, the selectivity indices were either reduced or could no longer be exactly determined. These data indicate that chloride complexes of gold(I) phosphines are the most promising as new agents against *T. vaginalis* with improved selectivity over human cells.

Inhibition of different TrxR isoforms by gold(I) phosphines

AF is a potent inhibitor of TrxR in *T. vaginalis* with an IC50 value of ~100 nM, suggesting that TrxR inhibition is an important mechanism of AF action in this and other protozoan parasites.[20, 30] Therefore, we investigated whether the improved activity of the best gold(I) complexes is related to a similar action mechanism. *T. vaginalis* has five different TrxR isoforms with different cellular locations [31] and variable degrees of amino acid identity (Fig. 5A), raising the possibility that they are not all equally sensitive to gold(I) compounds. Analysis by qPCR revealed that all five isoforms were expressed in several independently isolated clinical *T. vaginalis* strains grown *in vitro*. TrxRc (encoded by TVAG_474980) was by far the most highly expressed isoform in all strains (Fig. 5B). The next most highly expressed isoform was TrxRh2 encoded by TVAG_125360), followed by TrxRc2 (TVAG_348010), TrxRc3 (TVAG_240530), and TrxRh1 (TVAG_281360). Expression of these isoforms differed modestly between the different strains but was not consistently affected by resistance to Mz (Fig. 5B).

For cell-free drug testing, we had previously produced the most highly expressed TrxR isoform, TrxRc, as a recombinant protein [20] and confirmed its >99% purity in the present study (Fig. 5C). In addition, we produced the second most abundant isoform, TrxRh2, in *E. coli* and purified it to >99% purity by nickel/nitrilotriacetic acid affinity chromatography (Fig. 5C). The two TrxR isoforms were then tested in an *in vitro* activity assay for inhibition by our library of gold(I) complexes. Inhibitory activities (pIC50) varied over a 500-fold range and were highly correlated between the two TrxR isoforms with a slope of ~1 (Fig. 5D), indicating that their differences in amino acid sequences did not impact the interaction with the gold(I) complexes. Furthermore, the inhibitory activity of the different gold(I) complexes for each isoform displayed good correlation with the inhibition of total TrxR activity in whole-cell extracts of *T. vaginalis* (Fig. 5E). Notably, this correlation was lower than between the two isoforms, and inhibitory activities in whole-cell extracts spanned a more limited pIC50 range and showed a slope of <1 compared to the recombinant isoform assays, perhaps suggesting that other factors impact drug activity in the extracts. Correlation of inhibition of whole-cell TrxR activity (pIC50) in extracts with trichomonacidal activity

(pEC50) in live *T. vaginalis* revealed three distinct relationships: i) Eight of the compounds showed low activity against the live parasite regardless of their inhibitory activity against TrxR (Fig. 5F, gray dots); ii) ten compounds exhibited a significant correlation between pEC50 and pIC50, with about 10-fold lower activity against the live parasites compared to cell-free TrxR inhibition (Fig. 5F, black dots); and iii) four compounds displayed greater activity against live *T. vaginalis* compared to cell-free TrxR, so their ratios of pEC50:pIC50 were >1 (Fig. 5F, circle symbols with compound numbers). One of these compounds, **15**, had ~10-fold higher trichomonacidal activity than TrxR inhibitory activity. Together, these results are consistent with the notion that inhibition of TrxR isoform is one important mechanism-of-action of a subset of the gold(I) phosphines, but also suggest that other targets play a role in mediating the trichomonacidal activities of a different subset of gold(I) compounds.

Au(I) phosphines overcome 5-nitroheterocylic drug resistance in *T. vaginalis*

TrxR may be directly or indirectly involved in 5-nitroheterocylic drug resistance in protozoa[24, 32–34], which might compromise the effectiveness of gold(I) compounds in resistant cells. However, the expression analysis of TrxR isoforms had not revealed any consistent resistance-associated changes in expression (Fig. 5B), suggesting that they remain available as drug targets in resistant cells. To test this hypothesis, we used four Mz-resistant isolates of *T. vaginalis*, which were derived from patients who had failed Mz therapy.[35–37] The four lines exhibited a 20- to 100-fold loss in Mz susceptibility compared to four representative susceptible lines, confirming that resistance was stable and intrinsic to the parasites (Fig. 6A). All four lines were sensitive to two of the gold(I) complexes, **4** and **10**, as well as AF, with pEC50 values that were, on average, not significantly different from those in Mz-sensitive lines, although both Mz-sensitive and Mz-resistant lines showed a range of susceptibilities to the gold(I) compounds (Fig. 6A). Similar variations in the actions of the three gold(I) compounds were also observed in mammalian cytotoxicity for both transformed and non-transformed cells (Fig. 6A), although **4** retained its improved selectivity index of 8.6 on average, compared to 1.9 for AF, for all eight *T. vaginalis* lines over the mammalian cells. Furthermore, neither compound **4** nor AF interfered or synergized with the activity of Mz in a sensitive *T. vaginalis* strain (Fig. 6B), further underlining that the gold(I) complexes and Mz have different targets.

In vivo efficacy of gold(I) phosphines against vaginal trichomonad infection

To determine the *in vivo* efficacy of two of the most promising gold(I) compounds, **4** and **10**, we employed a murine model of trichomonad infection with *T. foetus*.[38] We first confirmed that both compounds, as well as AF as a control, were as active against *T. foetus in vitro* as they were against *T. vaginalis* (Fig. 7A). Subsequently, weanling female BALB/c mice were infected with *T. foetus* by intravaginal inoculation. After one day to allow establishment of the infection, mice were treated with five intravaginal doses of the gold(I) compounds over the ensuing three days (Fig. 7B), and infectious load was determined by direct parasite counting in vaginal washes. Both gold(I) compounds, **4** and **10**, either eliminated or at least markedly reduced infection (Fig. 7B), indicating that the two gold(I) phosphines were highly efficacious *in vivo*. Histological analysis confirmed the disappearance of *T. foetus*

trophozoites from the vaginal lumen after treatment with **4** (Fig. 7C). No clinically or histologically apparent adverse effects were observed with treatment (Fig. 7C).

DISCUSSION

Gold (I) compounds were first used in the 1940s as anti-inflammatory agents in the treatment of joint diseases. An orally active formulation, AF, was developed decades later in the 1980s for rheumatoid arthritis and remains the only available gold drug in the United States. Further development of gold(I) compounds has largely ceased since that time, presumably due to the significant adverse effects associated with the long-term use of the approved gold compounds.[23] Despite diminishing use as an anti-rheumatic agent, AF has recently experienced a potential renaissance as an antimicrobial agent with broad activities against a number of protozoal pathogens, including *E. histolytica*, *G. lamblia*, and *T. vaginalis*.[20–22, 24, 39] Antimicrobial properties were already noted for the earliest gold(I) compounds against mycobacteria, but this activity was not pursued clinically.[40] Part of the renewed hope for gold(I) compounds in antimicrobial therapy is that use in this indication would be short-term over days rather than long-term over months as required for the treatment of rheumatoid arthritis, since adverse effects often manifest over extended use. However, an alternative to this scenario is revealed in the present studies which indicate that gold(I) compounds can be developed with reduced toxicity and improved selectivity against at least one target pathogen, *T. vaginalis*. These findings raise the possibility that novel antimicrobial gold(I) compounds can predictably have diminished host toxicity for both pharmacokinetic reasons (reduced total exposure during short-term anti-infective therapy) and pharmacodynamic reasons (greater specificity for the pathogen over human cells), which are likely to act in synergistic fashion.

The mechanisms of action of gold(I) compounds are not fully understood, although a number of molecular targets have been identified, including TrxR and several kinases, and are likely to provide at least part explanations for the anti-inflammatory activity of these compounds.[41–43] Inactivation of these targets is presumed to occur by adduction of the gold(I) ion to critical sulfhydryl groups in the target protein[44], but this basic mechanism could not provide a ready explanation for the apparent selectivity of specific gold(I) complexes for *T. vaginalis* over human cells. It is possible that shedding of the phosphine and halide ligands from the gold(I) complex and formation of a new complex with thiol targets is context dependent and only occurs selectively when certain physical constraints are met in proximity to particular target molecules.[44, 45] Alternatively, particular gold(I) complexes may retain their phosphine ligands during adduct formation, in which case the physical binding requirements of the complex might be more restricted than those for the bare gold(I) ion, thereby potentially providing broader structural explanations for increased selectivity. The nature of the gold(I) adducts remain to be elucidated in *T. vaginalis*, but our results provide impetus for exploring differential target binding of the most selective gold(I) compounds.

All of the tested gold(I) complexes inhibited TrxR in *T. vaginalis*, with the most potent compounds exhibiting IC50 values of <50 nM, little difference in inhibition of two of the most abundantly expressed TrxR isoforms, and good correlations between inhibition of

individual isoforms and inhibition of total cellular TrxR activity. This inhibition is likely to contribute to the trichomonacidal actions of many of the gold(I) compounds, since it compromises critical anti-oxidant defenses in protozoan parasites.[46, 47] However, our data also suggest that TrxR isoforms are not the only targets of the gold(I) compounds, since we identified several compounds that were markedly (up to 10-fold) more active in killing whole cells than inhibiting TrxR activity. Other protein targets of AF have been identified in mammalian cells, such as signaling kinases,[48] phosphatases,[49] and metabolic enzymes,[50] and some of these have analogues in *T. vaginalis*.[51] In addition, replacement of the thiosugar ligand in gold(I) compounds with halide ligands, as done in our most promising compounds, can enhance reactivity toward oligonucleotides, thereby broadening the potential target range.[52] Intriguingly, two of the compounds with increased activity against whole cells compared to TrxR were gold(I) bisphosphines, suggesting opportunities for further combinatorial structural diversification. The specific targets of these and other selective gold(I) compounds in *T. vaginalis* are not known at present, but our findings provide the basis for identifying the targets as possible explanation for improved selectivity.

Several gold(I) compounds were shown to overcome resistance to Mz in *T. vaginalis*, indicating that their targets were not lost or altered in resistant cells. Consistent with independence of the targets for these two antimicrobial classes, we found that Mz and Au(I) compounds displayed no synergies in their activities even in Mz-sensitive cells. These findings may have two underlying reasons, depending on the presumed relative roles of TrxR in mediating the actions of the gold(I) compounds and resistance to Mz. If TrxR inhibition is indeed critical for gold(I) activity, as suggested by prior work[20, 21] and consistent with some of the present findings, it would indicate that the Mz resistance in none of the four separate Mz-resistant *T. vaginalis* lines is dependent on inactivation of TrxR, contrary to what had been suggested before.[12] Alternatively, if TrxR is truly important in Mz resistance, the findings would suggest that the gold(I) compounds had other critical targets in the parasite. The latter interpretation is consistent with our observation that several Au(I) compounds were more active against live *T. vaginalis* than TxR in enzymatic assays. In either case, our observations suggest that gold(I) compounds may be suitable as rescue therapy in patients with Mz-refractory trichomoniasis.

Treatment by topical administration of gold(I) compounds was shown to be effective in a murine vaginal trichomonad infection model. In contrast, both currently FDA-approved drugs, Mz and tinidazole, against trichomoniasis are given by the oral route. Intravaginal formulations of Mz do exist for other indications, but have shown only modest and variable efficacy for *T. vaginalis*.[53, 54] Nonetheless, topical drug treatment is possible in principle, as shown in murine infection models[55, 56] and further confirmed here, and is attractive, because low systemic absorption is likely to reduce systemic adverse effects, which in the case of Mz can involve metallic taste, nausea, dizziness, and general microbiome changes, as compared to oral formulations. In fact, intravaginal administration of Mz leads to a 96–98% decrease in systemic exposure compared to a single oral dose.[57] Similarly, we found recently that systemic exposure and adverse effects to AF can be significantly reduced by topical administration of a nanoformulation, while improving local efficacy.[56] The underlying nanotechnology is a broadly permissive formulation platform suitable for a wide range of hydrophilic and hydrophobic drugs and could thus be readily adapted to

improved gold(I) compounds, thus potentially acting synergistically by combining increased potency and selectivity with optimized topical pharmacokinetics.

CONCLUSIONS

Our structure-activity explorations demonstrate that diversification of gold(I) complexes, particularly as halides with simple trialkyl phosphines of C1-C3 chain length or as as bis(trialkyl phosphine) complexes can markedly improve potency against *T. vaginalis* and selectivity over human cells compared to the three FDA-approved but largely discontinued anti-rheumatic gold(I) drugs. All gold(I) complexes effectively inhibited the two most abundant isoforms of the presumed target enzyme, TrxR, but a subset of compounds were markedly more active against live *T. vaginalis* than TrxR, suggesting that alternative targets exist. Furthermore, all tested gold(I) complexes acted independently of Mz and were able to overcome Mz resistance, so they may be effective in the treatment of Mz-refractory trichomoniasis.

EXPERIMENTAL SECTION

General chemical methods

All chemicals were purchased from commercial sources and used without further purification, unless otherwise mentioned. Reactions were monitored by thin layer chromatography (TLC) using TLC plates precoated with TLC silica gel 60 F_{254} (Merck KGaA). Spots on TLC were visualized either directly with ultraviolet light or after staining with $KMnO_4$ stain. Where applicable, flash column chromatography was performed to isolate the compounds, with a suitable eluent determined by TLC. ^{1}H, ^{13}C-^{1}H, and ^{31}P-^{1}H NMR spectra were acquired on Varian Mercury 400, Varian 500S or Varian 600 instruments at 400.1, 500.1 and 600.1 MHz frequency for the proton channel of each instrument, respectively. All chemical shifts (δ) are quoted in ppm and all coupling constants (*J*) are expressed in Hertz (Hz). All NMR samples were prepared using $CDCl_3$. ^{1}H NMR and ^{13}C NMR chemical shifts were determined relative to the residual solvent signals. ^{31}P chemical shifts are referenced to an 85% phosphoric acid external standard. The following abbreviations are used for convenience in reporting the multiplicity for NMR resonances: s = singlet, d = doublet, dd = doublet of doublets, dt = doublet of triplets, t = triplet, td = triplet of doublets, q = quartet, br = broad signal, quint = quintet, and m = multiplet.

High resolution mass spectra were measured using Agilent 6545XT qToF instrument coupled with 1290 LC system. QToF mass spectrometer was equipped with an electrospray ionization source. Measurements were performed in positive ion mode with following ionization parameters: Capillary Voltage −4.5 kV, Nozzle Voltage 0 kV, nitrogen was applied as a nebulizer gas 35 psi, sheath gas 12 L × min^{-1}, 150 °C, dry gas 8 L × min^{-1}, 200 °C, and collision gas. Spectra were recorded in *m/z* 100 – 1700 range. For external calibration and tuning, a low-concentration tuning mix solution by Agilent Technologies was utilized. For sample injection (1 μL injection of *ca.* 10^{-6} M solution in MeCN/DCM) LC autosampler system was used: injected compounds were directly forwarded to the ionization source. All the MS spectra were recorded at 1 Hz. Spectra were processed using Agilent MassHunter

10.0 software package. Purity of compounds was determined by absolute quantitative 1D ^{1}H NMR (qHNMR). All the target compounds were ≧95% pure.

Synthesis of non-acetylated and peracetylated thioglucose–Au–PR_3 complexes (1) (5) (6).—For synthesis of all thioglucose–Au–PR_3, 1-Thio-β-D-glucose 2,3,4,6-tetraacetate was first synthesized using a modification of reported procedures.[29, 58]

For the non-acetylated thioglucose derivatives **1** and **6**, PR_3AuCl (13.8 μmol, 1.0 equiv.) was added to a screw cap vial, dissolved in MeOH (1mL), and cooled to 0 °C. In a separate screw cap vial, NaOMe (69 mmol, 5 equiv.) solution was prepared in MeOH (1.5 mL) and synthesized compound 1-Thio-β-D-glucose 2,3,4,6-tetraacetate (13.8 μmol, 1.0 equiv.) was dissolved in it. This solution was added dropwise to the cooled solution of PR_3AuCl. The reaction mixture was allowed to stir at room temperature for 1–2 h. To this reaction mixture, formic acid (300 μL) was added and separation of white precipitate was observed. Solvent was evaporated under reduced pressure and crude sample was placed overnight under vacuum. The crude product was taken up in DCM (2 mL) and filtered through Celite. Solvent was evaporated under reduced pressure to obtain the desired product. The resulting compounds had the following characteristics:

1 – (1-Thio-β-D-glucopyranosato) (triethylphosphine) gold(I); colorless viscous solid; yield 92%; ^{1}H NMR ($CDCl_3$, 600 MHz) δ 4.97 (d = 9.1 Hz, 1H), 3.87 (dd = 11.8, 3.5 Hz, 1H), 3.77 (dd = 11.8, 4.8 Hz, 1H), 3.60 – 3.51 (m, 2H), 3.40 – 3.44 (m, 1H), 3.34 – 3.18 (m, 5H), 1.79 – 1.91 (m, 6H), 1.14 – 1.27 (m, 9H); ^{13}C NMR ($CDCl_3$, 151 MHz) δ 85.46, 80.05, 79.72, 77.17, 71.10, 62.66, 17.94 (d = 34.5 Hz), 9.03; ^{31}P-^{1}H NMR ($CDCl_3$, 243 MHz) δ 36.96. ESI-MS (TOF): accurate *m/z* 825.1461; exact *m/z* calcd for $C_{18}H_{41}P_2O_5SAu_2$ [2M–$C_6H_{11}O_5S$]$^{+}$ 825.1475 (Δ = 1.7 ppm).

6 – (1-Thio-β-D-glucopyranosato) (tributylphosphine) gold(I); colorless viscous solid; yield 52%; ^{1}H NMR ($CDCl_3$, 500 MHz) δ 4.98 (d = 9.0 Hz, 1H), 3.89 (dd = 11.7, 3.7 Hz, 1H), 3.78 (dd = 11.8, 4.8 Hz, 1H), 3.62 – 3.52 (m, 2H), 3.41 – 3.46 (m, 1H), 3.23 (t = 8.6 Hz, 1H), 2.79 (br), 1.88 –1.76 (m, 6H), 1.59 – 1.43 (m, 12H), 0.95 (t = 7.2 Hz, 9H); ^{13}C-^{1}H NMR ($CDCl_3$, 126 MHz) δ 85.66, 79.92, 79.77, 77.21, 71.42, 62.96, 27.23, 25.45 (d = 33.2 Hz), 24.10 (d = 14.6 Hz), 13.65; ^{31}P-^{1}H NMR ($CDCl_3$, 202 MHz) δ 26.64. ESI-MS (TOF): accurate *m/z* 993.3340; exact *m/z* calcd for $C_{30}H_{65}P_2O_5SAu_2$ [2M–$C_6H_{11}O_5S$]$^{+}$ 993.3353 (Δ = 1.3 ppm).

For the peracetylated thioglucose derivative **5**, PR_3AuCl (58 μmol, 1.0 equiv.) was added to a screw cap vial and dissolved in EtOH (1mL) and the solution was cooled to 0 °C. Another screw cap vial was charged with the synthesized compound 1-Thio-β-D-glucose 2,3,4,6-tetraacetate (58 μmol, 1.0 equiv.) and EtOH (1 mL) was added. NaOH (53 μmol, 0.9 equiv.) was added and 1-Thio-β-D-glucose 2,3,4,6-tetraacetate dissolved over a few minutes while stirring. This solution was added dropwise to the cooled solution of PR_3AuCl and the reaction mixture was allowed to stir at 0 °C for 1–2 h. The reaction was monitored for completion. Solvent was evaporated under reduced pressure to obtain the crude compound. The solid was taken up in DCM and filtered through Celite, concentrated

under reduced pressure to obtain the desired product. The resulting compound had the following characteristics:

5 – (2,3,4,6-Tetra-O-acetyl-1-thio-*β*-D-galacotopyranosato)(butylphosphine) gold(I); colorless viscous liquid; yield 85%; ^{1}H NMR ($CDCl_3$, 500 MHz) δ 5.17 – 5.04 (m, 3H), 4.97 (t = 9.3 Hz, 1H), 4.22 (dd = 12.2, 5.0 Hz, 1H), 4.09 (dd = 12.2, 2.4 Hz, 1H), 3.67 – 3.73 (m, 1H), 2.06 (s, 3H), 2.05 (s, 3H), 2.00 (s, 3H), 1.96 (s, 3H), 1.74 – 1.82 (m, 6H), 1.61 – 1.52 (m, 6H), 1.46 (h = 7.2 Hz, 6H), 0.94 (t = 7.2 Hz, 9H); ^{13}C-^{1}H NMR ($CDCl_3$, 126 MHz) δ 170.77, 170.29, 169.55, 169.54, 83.29, 77.48, 75.69, 74.28, 68.95, 62.91, 27.20, 25.54 (d = 33.4 Hz), 24.10 (d = 14.4 Hz), 21.12, 20.80, 20.64, 20.62, 13.62; ^{31}P-^{1}HHH NMR ($CDCl_3$, 202 MHz) δ 27.79. ESI-MS (TOF): accurate *m/z* = 763.2329; exact *m/z* calcd for $C_{26}H_{47}O_9SPAu$ $[M+H]^+$ = 763.2338 (Δ = 1.2 ppm).

Synthesis of Thiomalic acid–Au–PR$_3$ complexes (2) (7).—Thiomalic acid–Au–PR_3 complexes were synthesized using reported procedure.[59] Thiomalic acid (0.11 mmol, 1.0 equiv.) was dissolved in aq. NaOH (0.34 mmol, 3.0 equiv. in 1mL H_2O) and the solution was cooled to 0 °C. PR_3AuCl (0.11 mmol, 1.0 equiv.) was dissolved in cold EtOH (1.5 mL) and thiomalic solution was added to this dropwise. The reaction mixture was stirred for 2 h while maintaining the temperature below 0 °C and then formic acid (0.15 ml) was added while stirring. Solvent was evaporated under reduced pressure and the compound was resuspended in DCM (3 mL). Insoluble sodium formate was filtered out and the organic layer was separated and concentrated under reduced pressure to obtain the product. The resulting compounds had the following characteristics:

2 – *S*-Triethylphosphine gold(I) thiomalic acid; white solid; yield 97%; ^{1}H NMR ($CDCl_3$, 600 MHz) δ 4.17 (s, 1H), 3.04 – 2.75 (m, 2H), 1.95 – 1.79 (m, 6H), 1.13 – 1.27 (m, 9H); ^{13}C-^{1}H NMR ($CDCl_3$, 151 MHz) δ 181.40, 176.22, 44.15, 40.54, 17.78 (d = 31.1 Hz), 9.00; ^{31}P-^{1}H NMR ($CDCl_3$, 243 MHz) δ 36.03. ESI-MS (TOF): accurate *m/z* = 465.0577; exact *m/z* calcd for $C_{10}H_{21}PO_4SAu$ $[M+H]^+$ 465.0558 (Δ = 4.1 ppm).

7 – *S*-Tributylphosphine gold(I) thiomalic acid; white solid; yield 88%; ^{1}H NMR ($CDCl_3$, 600 MHz) δ 4.28 (t = 6.4 Hz, 1H), 3.00 – 2.91 (m, 2H), 1.85 – 1.78 (m, 6H), 1.59 – 1.52 (m, 6H), 1.47 (h = 7.8 Hz, 6H), 0.94 (t = 7.3 Hz, 9H); ^{13}C-^{1}H NMR ($CDCl_3$, 126 MHz) δ 180.31, 175.28, 43.75, 41.20, 27.07, 25.22 (d = 32.8 Hz), 24.10 (d = 13.6 Hz), 13.65; ^{31}P-^{1}H NMR ($CDCl_3$, 202 MHz) δ 26.18. ESI-MS (TOF): accurate *m/z* = 549.1500; exact *m/z* calcd for $C_{16}H_{33}PO_4SAu$ $[M+H]^+$ 549.1497 (Δ = 0.6 ppm).

Synthesis of NHC–Au–PR$_3$ complexes (3) (8).—NHC–Au–PR_3 complexes were synthesized using a modification of reported procedure.[60] The 1,3-bis(2,4,6-trimethylphenyl)imidazolium chloride (0.11mmol, 1.0 equiv.) was treated with PR_3AuCl (0.11 mmol, 1.0 equiv.) in the presence of K_2CO_3 (0.11 mmol, 1.0 equiv.) under vigorous stirring for 24 h in DCM/water biphasic mixture (2 mL DCM, 1mL H_2O) at room temperature. The organic layer was separated and was concentrated under reduced pressure. Crude mixture was purified using flash chromatography (SiO_2) with DCM/MeOH solvent system to obtain the desired product. The resulting compounds had the following characteristics:

3 – [Triethylphosphine-(bis(2,4,6-trimethylphenyl)imidazol-2-ylidene)]gold(I) chloride; white crystalline solid; yield 65%; ^{1}H NMR ($CDCl_3$, 600 MHz) δ 7.42 (s, 4H), 7.03 (s, 2H), 2.35 (s, 6H), 2.10 (s, 12H), 1.68 – 1.75 (m, 6H), 0.88 – 0.81 (m, 9H); ^{13}C-^{1}H NMR (151 MHz, Chloroform-*d*) δ 191.43 (d = 123.2 Hz), 140.37, 134.56, 133.96, 129.43, 123.71, 21.10, 17.69, 17.48, 9.05; ^{31}P-^{1}H NMR ($CDCl_3$, 243 MHz) δ 40.29. ESI-MS (TOF): accurate *m/z* 619.2516; exact *m/z* calcd for $C_{27}H_{39}PN_2Au$ $[M–Cl]^+$ 619.2511 (Δ = 0.8 ppm).

8 – [Tributylphosphine-(bis(2,4,6-trimethylphenyl)imidazol-2-ylidene)]gold(I) chloride; white viscous solid; yield 70%; ^{1}H NMR ($CDCl_3$, 600 MHz) δ 7.50 (s, 4H), 7.03 (s, 2H), 2.35 (s, 6H), 2.11 (s, 12H), 1.67 – 1.59 (m, 6H), 1.29 – 1.23 (m, 6H), 1.19 – 1.12 (m, 6 H), 0.82 (t = 7.3 Hz, 9H); ^{13}C-^{1}H NMR ($CDCl_3$, 151 MHz) δ 190.39 (d = 123.7) , 140.14, 134.59, 134.07, 129.40, 124.10 (d = 2.7 Hz), 27.52, 25.09 (d = 33.6 Hz), 23.77 (d = 13.5 Hz), 21.12, 17.71, 13.58; ^{31}P-^{1}H NMR ($CDCl_3$, 243 MHz) δ 28.72. ESI-MS (TOF): accurate *m/z* 703.3458; exact *m/z* calcd for $C_{33}H_{51}PN_2Au$ $[M–Cl]^+$ 703.3450 (Δ = 1.1 ppm).

Synthesis of PR_3–Au–Cl complexes (9) (11) (12) (18).—PR_3–Au–Cl complexes were synthesized using (dimethylsulfide)gold(I) chloride [$(Me_2S)AuCl$] and the corresponding commercially purchased PR_3. In a screw cap vial, $(Me_2S)AuCl$ (0.17 mmol, 1.0 equiv.) was dissolved in dry THF (1.5 mL) inside a nitrogen-filled glove box at room temperature. To a stirred solution, PR_3 (0.19 mmol, 1.1 equiv.) was added dropwise. The mixture was stirred overnight and moved out of the glovebox. THF was evaporated under reduced pressure. The solid was dissolved in 2.5 mL dichloromethane (DCM) and passed through a short pad of silica and Na_2SO_4. The eluted solution was concentrated under nitrogen flow. The resulting compounds had the following characteristics:

9 – (Tri-*n*-butylphosphine)gold(I) chloride; colorless viscous oil; yield 66%; ^{1}H NMR ($CDCl_3$, 500 MHz) δ 1.84 – 1.72 (m, 2H), 1.62 – 1.51 (m, 2H), 1.50 – 1.41 (m, 2H), 0.93 (t = 7.2 Hz, 3H); ^{13}C-^{1}H NMR ($CDCl_3$, 126 MHz) δ 27.28, 25.59 (d = 36.3 Hz), 24.03 (d = 14.8 Hz), 13.59; ^{31}P-^{1}H NMR ($CDCl_3$, 202 MHz) δ 22.08. ESI-MS (TOF): accurate *m/z* 399.1506; exact *m/z* calcd for $C_{12}H_{27}PAu$ $[M–Cl]^+$ 399.1510 (Δ = 1.0 ppm).

11 – (Tri-*n*-propylphosphine)gold(I) chloride; yellow viscous liquid; yield 95%; NMR data: ^{1}H NMR ($CDCl_3$, 400 MHz) δ 1.80 – 1.74 (m, 6H), 1.67 – 1.59 (m, 6H), 1.08 (t = 7.2 Hz, 9H); ^{13}C-^{1}H NMR ($CDCl_3$, 101 MHz) δ 28.09 (d = 36.1 Hz), 18.98, 15.61 (d = 15.7 Hz); ^{31}P-^{1}H NMR ($CDCl_3$, 202 MHz) δ 20.72. ESI-MS (TOF): accurate *m/z* 357.1038; exact *m/z* calcd for $C_9H_{21}PAu$ $[M–Cl]^+$ 357.1041 (Δ = 0.9 ppm).

12 – (Triisopropylphosphine)gold(I) chloride; white needle like crystals; yield 51%; ^{1}H NMR ($CDCl_3$, 600 MHz) δ 2.28 (dt = 9.5, 7.2 Hz, 1H), 1.31 (dd = 16.2, 7.2 Hz, 6H); ^{13}C-^{1}H NMR ($CDCl_3$, 101 MHz) δ 23.94 (d = 31.3 Hz), 20.28; ^{31}P-^{1}H NMR ($CDCl_3$, 162 MHz) δ 64.27. ESI-MS (TOF): accurate *m/z* 357.1033; exact *m/z* calcd for $C_9H_{21}PAu$ $[M–Cl]^+$ 357.1041 (Δ = 2.2 ppm).

18 – (Dimethylphenylphosphine)gold(I) chloride; whitish viscous liquid; yield 87%; ^{1}H NMR ($CDCl_3$, 600 MHz) δ 7.79 – 7.74 (m, 2H), 7.53 – 7.49 (m, 3H), 1.95 – 1.88 (m, 6H); ^{13}C-^{1}H NMR ($CDCl_3$, 101 MHz) δ 131.78, 131.68, 131.61, 129.118, 129.17 (d = 7.8 Hz),

15.61 (d = 35.3 Hz); ^{31}P-^{1}H NMR ($CDCl_3$, 243 MHz) δ 9.08. ESI-MS (TOF): accurate *m/z* 335.0256; exact *m/z* calcd for $C_8H_{11}PAu$ $[M–Cl]^+$ 335.0258 (Δ = 0.6 ppm).

Synthesis of [PR"$_3$–Au–PR$_3$]Cl complexes (13) (14) (15) (16).—[PR"$_3$–Au–PR$_3$]Cl complexes were synthesized using the commercial or previously synthesized PR_3AuCl complex. In a screw cap vial, PR_3AuCl (0.17 mmol, 1.0 equiv.) was dissolved in dry THF (1.5 mL) inside a nitrogen-filled glove box at room temperature. To a stirred solution, THF solution of commercially purchased PR"$_3$ (0.34 mmol, 1.1 equiv.) was added. The mixture was allowed to stir overnight and moved out of the glovebox. Reaction mixture was transferred to a screw cap vial with DCM. Solvents were evaporated under reduced pressure to obtain the crude product. The crude product was purified using flash chromatography (SiO_2) with a DCM/MeOH solvent system. The resulting compounds had the following characteristics:

13 – Bis(trimethylphosphine)gold(I) chloride; white amorphous solid; yield 75%; ^{1}H NMR ($CDCl_3$, 600 MHz) δ 1.63 (s, 1H); ^{13}C-^{1}H NMR ($CDCl_3$, 151 MHz) δ 15.73; ^{31}P-^{1}H NMR ($CDCl_3$, 243 MHz) δ 2.94. ESI-MS (TOF): accurate *m/z* 349.0538; exact *m/z* calcd for $C_6H_{18}P_2Au$ $[M–Cl]^+$ 349.0544 (Δ = 1.7 ppm).

14 – Bis(triethylphosphine)gold(I) chloride; shiny white crystals; yield 83%; ^{1}H NMR ($CDCl_3$, 400 MHz) δ 2.00 (q = 7.6 Hz, 2H), 1.21 (t = 7.7 Hz, 3H); ^{13}C-^{1}H NMR ($CDCl_3$, 101 MHz) δ 17.31, 8.91; ^{31}P-^{1}H NMR ($CDCl_3$, 162 MHz) δ 41.95. ESI-MS (TOF): accurate *m/z* 433.1486; exact *m/z* calcd for $C_{12}H_{30}P_2Au$ $[M–Cl]^+$ 433.1483 (Δ = 0.7 ppm).

15 – Bis(tri-*n*-propylphosphine)gold(I) chloride; colorless liquid; yield 80%; ^{1}H NMR ($CDCl_3$, 600 MHz) δ 1.84 – 1.91 (m, 2H), 1.66 – 1.46 (m, 2H), 1.03 (t = 7.3 Hz, 3H); ^{13}C-^{1}H NMR ($CDCl_3$, 101 MHz) δ 27.28 (d = 28.4 Hz), 18.58, 15.72 (d = 13.3 Hz); ^{31}P-^{1}H NMR ($CDCl_3$, 243 MHz) δ 29.90. ESI-MS (TOF): accurate *m/z* 517.2430; exact *m/z* calcd for $C_{18}H_{42}P_2Au$ $[M–Cl]^+$ 517.2422 (Δ = 1.5 ppm).

16 – Bis(triisopropylphosphine)gold(I) chloride; colorless crystals; yield 73%; ^{1}H NMR ($CDCl_3$, 600 MHz) δ 2.77 – 2.37 (m, 1H), 1.36 (d = 7.7 Hz, 6H); ^{13}C-^{1}H NMR ($CDCl_3$, 151 MHz) δ 24.16, 20.50; ^{31}P-^{1}H NMR ($CDCl_3$, 243 MHz) δ 73.05. ESI-MS (TOF): accurate *m/z* 517.2450; exact *m/z* calcd for $C_{18}H_{42}P_2Au$ $[M–Cl]^+$ 517.2422 (Δ = 5.4 ppm).

Synthesis of PR$_3$–Au–Br complexes (23) (24).—PR_3–Au–Br complexes were synthesized using a modification of the reported procedure.[61] To an ethanolic solution of PR_3AuCl (57 μmol, 1.0 equiv., 1 mL), an aqueous solution of $AgNO_3$ (57 μmol, 1.0 equiv., 1mL) was added dropwise under atmospheric conditions. The precipitated AgCl was removed by vacuum filtration. The colorless, aqueous solution of $[Au(H_2O)(PR_3)]NO_3$ was treated with aqueous NaBr solution (1.5 equiv., 1.2 mL) to obtain solid $AuBr(PR_3)$. The solid was filtered out and washed with H_2O (1.5 mL). The solid obtained was dried and treated with DCM (2 mL). The solution was passed through a short pad of silica and Na_2SO_4, eluting with DCM. The eluted solution was dried under nitrogen flow to obtain crystalline solid product. The resulting compounds had the following characteristics:

23 – (Trimethylphosphine)gold(I) bromide; pale yellow needle-like crystals; yield 60%; NMR data: ^{1}H NMR ($CDCl_3$, 600 MHz) δ 1.61 (d = 11.2 Hz, 9H); ^{13}C-^{1}H NMR ($CDCl_3$, 101 MHz) δ 16.15 (d = 39.3 Hz); ^{31}P-^{1}HH NMR ($CDCl_3$, 243 MHz) δ −6.20. ESI-MS (TOF): accurate *m/z* 273.0096; exact *m/z* calcd for C_3H_9PAu $[M–Br]^+$ 273.0102 (Δ = 2.2 ppm).

24 – (Triethylphosphine)gold(I) bromide; shiny white crystals; yield 79%; NMR data: ^{1}H NMR ($CDCl_3$, 600 MHz) δ 1.85 (dq = 10.3, 7.6 Hz, 6H), 1.21 (dt = 19.0, 7.7 Hz, 9H); ^{13}C-^{1}H NMR ($CDCl_3$, 101 MHz) δ 18.19 (d = 35.4 Hz), 8.91; ^{31}P-^{1}H NMR ($CDCl_3$, 243 MHz) δ 34.30. ESI-MS (TOF): accurate *m/z* 315.0564; exact *m/z* calcd for $C_6H_{15}PAu$ $[M–Br]^+$ 315.0571 (Δ = 2.2 ppm).

Synthesis of PR_3-Au-I complexes (25) (26).—PR_3–Au–I complexes were synthesized using a modification of reported procedures.[52, 62] PR_3AuCl (57 μmol, 1.0 equiv.) was dissolved in 1 mL acetone (when R=Me) or ethanol (when R= Et), sodium iodide (0.29 mmol, 5.0 equiv.) was added under atmospheric conditions and stirred overnight. The reaction mixture was passed through a syringe filter. The filtrate was concentrated under reduced pressure. The solid obtained was suspended in a mixture of EtOH/hexanes (1:9) and passed through a short pad of silica and Na_2SO_4. The organic phase was concentrated under nitrogen flow to obtain a crystalline product. The resulting compounds had the following characteristics:

25 – (Trimethylphosphine)gold(I) iodide; white amorphous solid; yield 50%; NMR data: ^{1}H NMR ($CDCl_3$, 600 MHz) δ 1.59 (d = 11.0 Hz, 9H); ^{13}C-^{1}H NMR ($CDCl_3$, 101 MHz) δ 16.17 (d = 37.1 Hz); ^{31}P-^{1}H NMR ($CDCl_3$, 243 MHz) δ 1.63. ESI-MS (TOF): accurate *m/z* 273.0096; exact *m/z* calcd for C_3H_9PAu $[M–I]^+$ 273.0102 (Δ = 2.2 ppm).

26 – (Triethylphosphine)gold(I) iodide; pale yellow amorphous solid; yield 53%; NMR Data: ^{1}H NMR ($CDCl_3$, 600 MHz) δ 1.87 (dq = 10.1, 7.7 Hz, 6H), 1.23 (dt = 18.8, 7.6 Hz, 9H); ^{13}C-^{1}H NMR ($CDCl_3$, 101 MHz) δ 18.32 (d = 33.7 Hz), 8.80; ^{31}P-^{1}H NMR ($CDCl_3$, 243 MHz) δ 39.56. ESI-MS (TOF): accurate *m/z* 315.0564; exact *m/z* calcd for $C_6H_{15}PAu$ $[M–I]^+$ 315.0571 (Δ = 2.2 ppm).

Other gold(I) complexes.—The following gold(I) complexes were purchased: Auranofin – 2,3,4,6-Tetra-O-acetyl-1-thio-*β*-D-galacotopyranosato)(ethylphosphine) gold(I) (Enzo Life Sciences, Cat No BML-EI206); Aurothioglucose (brand name: Solganal) – 3,4,5-trihydroxy-6-(hydroxymethyl)oxane-2-thiolate gold (I) (Millipore Sigma, Cat No A0606); Aurothiomalate (brand name: Myochrysine) – (1,2-Dicarboxyethylthio) disodium salt hydrate gold(I) (Millipore Sigma, Cat No 157201); **4** – (Tri-*n*-ethylphosphine)gold(I) chloride (Millipore Sigma, Cat No 288225); **10** – (Tri-*n*-methylphosphine)gold(I) chloride (Strem Chemicals, Cat No 79–0850); **17** – (Tri-*tert*-butylphosphine)gold(I) chloride (Strem Chemicals, Cat No 79–0740); **19** – (Methyldiphenylphosphine)gold(I) chloride (Millipore Sigma, Cat No 717290); **20** – (Triphenylphosphine)gold(I) chloride (Millipore Sigma, Cat No 254037); **21** – [Tri(*p*-tolyl)phosphine]gold(I) chloride (Millipore Sigma, Cat No 717282); and **22** – [Tris(para-trifluoromethylphenyl)phosphine]gold(I) chloride (Millipore Sigma, Cat No 665177).

Trichomonad cultures and drug assays.—The following trichomonad strains were used in the studies: *T. vaginalis* G3 (ATCC PRA-98), F1623,[63] *T. vaginalis* LA1,[64] *T. vaginalis* B7268,[37] *T. vaginalis* B4407 (kindly provided by Dr. Jacqueline Upcroft, Queensland Institute of Medical Research), *T. vaginalis* S1469, *T. vaginalis* MSA1171, *T. vaginalis* MSA1141, *T. vaginalis* R88, *T. vaginalis* R93 (kindly provided by Dr. Evan Secor, US Centers for Disease Control and Prevention), and *T. foetus* D1.[38] Trichomonads were grown at 37 °C in TYM Diamond's medium supplemented with 180 μM ferrous ammonium sulphate.[65] Drug susceptibility assays were performed as described previously.[66] Briefly, stocks of the test compounds were diluted in phosphate-buffered saline to 75 μM, and 1:3 serial dilutions were made. Trophozoites (5×10^3/well) were added to the wells in 96-well plates and cultures were grown for 24 h at 37 °C under anaerobic conditions (AnaeroPackTM-Anaero System; Remel). Growth and viability were determined with an ATP assay by adding BacTiter-GloTM Microbial Cell Viability Assay reagent (Promega) and measuring ATP-dependent luminescence in a microplate reader. The 50% effective concentration (EC50) was derived from the concentration–response curves using Graphpad prism (Graphpad Software).

Cytotoxicity assay in mammalian cells.—The human epithelial cell line, HeLa (ATCC CCL-2), the human epithelial-like liver cell line, HepG2 (ATCC HB-8065), and the non-transformed canine kidney epithelial cell line, MDCK (ATCC CCL-34), were used to determine drug cytotoxicity in mammalian cells. Compounds were serially diluted (1:3) and added to HeLa cell cultures in 96-well plates. The cells were grown for 48 h at 37 °C in 5% CO_2, 95% air, and viable-cell numbers were determined using BacTiter-GloTM Microbial Cell Viability Assay reagent.

Sequence alignments.—*T. vaginalis* possesses five different TrxR isotypes: TrxRc (TrxR_96723, 96723.m00098, gene *TVAG_474980*), TrxRh2 (TrxR_84394, 84394.m00089, gene *TVAG_125360*), TrxRc2 (TrxR_92349, 92349.m00258, gene *TVAG_348010*), TrxRc3 (TrxR_88289, 88289.m00178, gene *TVAG_240530*), TrxRh1 (TrxR_89667, 89667.m00077, gene *TVAG_281360*).[31] Amino acid sequences were aligned by ClustalW (v 1.83)[67] and dendrograms were generated by neighbor-joining method using MEGA[68] with *Giardia lamblia* TrxR (AJ507833) as a root.

Expression analysis.—Total RNA from trophozoites was isolated with TRIzol Reagent (Thermo Fisher) and reverse-transcribed into cDNA using the High Capacity cDNA Reverse Transcription kit (Applied Biosystems). Quantitative RT-PCR (qRTPCR) analysis was done with Mesa Green 2 x SYBR mix (Eurogentec) in a real-time PCR machine. Primers and expected PCR product size were: TrxRc 5'-CCC TCC CAA TGA GAA AGC GT-3', 5'-CTG TGT CTC GCC TGT CTT GT-3', 131 bp; TrxRh2 5'-CCA CAG AAG CAG GAG CTG AA-3', 5'-ACG ATA ACA GAG CGT GCC TT-3', 118 bp; TrxRc3 5'-CTG CTG TAG CGG TGT GTT CA-3', 5'- CTC CAG CGA CAA AAA CAC CC-3', 143 bp; TrxRh1 5'-TGC TAG AGC GGC ACT GAA A −3', 5'-GCT GTC GCT TGC GTT TGT AT-3', 144 bp; TrxRc2 5'-TCG CCG CTG AAG AAG CAT TA-3', 5'-TGG GTT GGA AGC ACG AAG T-3', 89 bp; GAPDH (*TVAG_366380*) 5'-TGC CGC AAG CTC TAT CCA AA-3',

5’-GCA CGG TGA GCT GTA TCG TA-3’, 104 bp. Relative changes in target mRNA levels were calculated by the $2^{\Delta\Delta Ct}$ method, with GAPDH mRNA as the reference standard.

Production and purification of recombinant TrxR.—Sequences of the *T. vaginalis* TrxRc and TrxRh2 isoforms were obtained from EuPathDB (https://eupathdb.org/eupathdb/Genes). The corresponding DNAs were generated by gene synthesis and inserted into NdeI-XhoI cloning sites of the bacterial expression vector pET-15b (Genescript). Following vector transformation into T7 Express lysY/Iq Competent *E. coli* (NEB), recombinant protein synthesis was induced by isopropyl β-d-1-thiogalactopyranoside (IPTG), and proteins were purified by Ni-NTA affinity chromatography (QIAGEN). Recombinant proteins were analyzed for purity by polyacrylamide gel electrophoresis (PAGE) and Coomassie staining.

TrxR activity assays.—TrxR activity was assayed in 100 mM potassium phosphate buffer (pH 7.0) containing the substrates 5,5-dithio-bis-(2-nitrobenzoic acid) (DTNB) (1 mM) and NADPH (0.2 mM). DTNB conversion to 2-nitro-5-thiobenzoic acid was determined by absorbance measurements at 420 nm.[16, 20] As controls, assays were performed with substrates but without TrxR, and with TrxR but without substrates.

Murine trichomonad infection model.—*In vivo* efficacy was determined in murine models as described previously.[38] Briefly, weanling (3- to 4-week-old) female BALB/cJ mice were inoculated intravaginally 10^6 x *T. foetus* D1 trophozoites. After one day, mice were given 5 μl per dose of 1% of the respective test compound in 0.1% hypromellose, or vehicle controls, intravaginally five times. On day 4, live trophozoites were enumerated in vaginal washes. For histological analysis, vaginal tissue was snap-frozen in OCT compound (Sakura Finetek), frozen sections (10 μm) were prepared and fixed in methanol for 10 min at room temperature, and stained with Wright-Giemsa stain. Bright-field images were taken with a 12 MP digital camera on an Eclipse 50i microscope (Nikon). All animal studies were reviewed and approved by the Institutional Animal Care and Use Committee of the University of California, San Diego, and were conducted in compliance with the guidelines of the Committee.

Data analysis.—For *in vitro* drug testing, experiments were repeated at least three times, and mean and S.E.M. of the $\log_{10}$-transformed half-maximal inhibition values were calculated. Significance were evaluated by unpaired T-test or ANOVA with Dunnett’s post-hoc test. For *in vivo* drug efficacy tests, groups of ≥7 animals were analyzed for trophozoite load per animal. Data are shown as individual data points along with the geometric mean for each group. Differences between groups were analyzed for significance ($P < 0.01$) by Kruskal-Wallis test using Graphpad prism (Graphpad software).

Supplementary Material

Refer to Web version on PubMed Central for supplementary material.

ACKNOWLEDGMENT

We thank Elaine Hanson and Christine Le for excellent technical support. The work was supported by NIH grants AI119459, AI146387, and DK120515, and a Takeda Science Foundation Grant (S. Ihara).

ABBREVIATIONS USED

AF	auranofin
ATG	aurothioglucose
ATM	aurothiomalate
Mz	metronidazole
MzR	metronidazole-resistant
MzS	metronidazole-sensitive
NHC	N-heterocyclic carbine
TrxR	thioredoxin reductase

REFERENCES

(1). Poole DN; McClelland RS Global epidemiology of Trichomonas vaginalis. Sex Transm Infect 2013, 89 (6), 418–422. [PubMed: 23744960]

(2). Marous M; Huang WY; Rabkin CS; Hayes RB; Alderete JF; Rosner B; Grubb RL 3rd; Winter AC; Sutcliffe S Trichomonas vaginalis infection and risk of prostate cancer: associations by disease aggressiveness and race/ethnicity in the PLCO Trial. Cancer Causes Control 2017, 28 (8), 889–898. [PubMed: 28669054]

(3). Yang S; Zhao W; Wang H; Wang Y; Li J; Wu X Trichomonas vaginalis infection-associated risk of cervical cancer: A meta-analysis. Eur J Obstet Gynecol Reprod Biol 2018, 228, 166–173. [PubMed: 29980111]

(4). Kissinger P Epidemiology and treatment of trichomoniasis. Curr Infect Dis Rep 2015, 17 (6), 484. [PubMed: 25925796]

(5). Kissinger P Trichomonas vaginalis: a review of epidemiologic, clinical and treatment issues. BMC Infect Dis 2015, 15, 307. [PubMed: 26242185]

(6). Bolumburu C; Zamora V; Munoz-Algarra M; Portero-Azorin F; Escario JA; Ibanez-Escribano A Trichomoniasis in a tertiary hospital of Madrid, Spain (2013–2017): prevalence and pregnancy rate, coinfections, metronidazole resistance, and endosymbiosis. Parasitol Res 2020, 119 (6), 1915–1923. [PubMed: 32405804]

(7). Upcroft JA; Dunn LA; Wal T; Tabrizi S; Delgadillo-Correa MG; Johnson PJ; Garland S; Siba P; Upcroft P Metronidazole resistance in Trichomonas vaginalis from highland women in Papua New Guinea. Sex Health 2009, 6 (4), 334–338. [PubMed: 19917203]

(8). Lauwaet T; Miyamoto Y; Ihara S; Le C; Kalisiak J; Korthals KA; Ghassemian M; Smith DK; Sharpless KB; Fokin VV; Eckmann L Click chemistry-facilitated comprehensive identification of proteins adducted by antimicrobial 5-nitroimidazoles for discovery of alternative drug targets against giardiasis. PLoS Negl Trop Dis 2020, 14 (4), e0008224. [PubMed: 32302296]

(9). Kulda J; Tachezy J; Cerkasovova A In vitro induced anaerobic resistance to metronidazole in Trichomonas vaginalis. J Eukaryot Microbiol 1993, 40 (3), 262–269. [PubMed: 8508165]

(10). Rasoloson D; Vanacova S; Tomkova E; Razga J; Hrdy I; Tachezy J; Kulda J Mechanisms of in vitro development of resistance to metronidazole in Trichomonas vaginalis. Microbiology 2002, 148 (Pt 8), 2467–2477. [PubMed: 12177340]

(11). Hrdy I; Cammack R; Stopka P; Kulda J; Tachezy J Alternative pathway of metronidazole activation in Trichomonas vaginalis hydrogenosomes. Antimicrob Agents Chemother 2005, 49 (12), 5033–5036. [PubMed: 16304169]

(12). Leitsch D; Kolarich D; Binder M; Stadlmann J; Altmann F; Duchene M Trichomonas vaginalis: metronidazole and other nitroimidazole drugs are reduced by the flavin enzyme thioredoxin

reductase and disrupt the cellular redox system. Implications for nitroimidazole toxicity and resistance. Mol Microbiol 2009, 72 (2), 518–536. [PubMed: 19415801]

(13). Leitsch D; Drinic M; Kolarich D; Duchene M Down-regulation of flavin reductase and alcohol dehydrogenase-1 (ADH1) in metronidazole-resistant isolates of Trichomonas vaginalis. Mol Biochem Parasitol 2012, 183 (2), 177–183. [PubMed: 22449940]

(14). Leitsch D; Kolarich D; Duchene M The flavin inhibitor diphenyleneiodonium renders Trichomonas vaginalis resistant to metronidazole, inhibits thioredoxin reductase and flavin reductase, and shuts off hydrogenosomal enzymatic pathways. Mol Biochem Parasitol 2010, 171 (1), 17–24. [PubMed: 20093143]

(15). Leitsch D; Janssen BD; Kolarich D; Johnson PJ; Duchene M Trichomonas vaginalis flavin reductase 1 and its role in metronidazole resistance. Mol Microbiol 2014, 91 (1), 198–208. [PubMed: 24256032]

(16). Coombs GH; Westrop GD; Suchan P; Puzova G; Hirt RP; Embley TM; Mottram JC; Muller S The amitochondriate eukaryote Trichomonas vaginalis contains a divergent thioredoxin-linked peroxiredoxin antioxidant system. J Biol Chem 2004, 279 (7), 5249–5256. [PubMed: 14630923]

(17). Goodhew EB; Secor WE Drug library screening against metronidazole-sensitive and metronidazole-resistant Trichomonas vaginalis isolates. Sex Transm Infect 2013, 89 (6), 479–484. [PubMed: 23794105]

(18). Urbanski LJ; Di Fiore A; Azizi L; Hytonen VP; Kuuslahti M; Buonanno M; Monti SM; Angeli A; Zolfaghari Emameh R; Supuran CT; De Simone G; Parkkila S Biochemical and structural characterisation of a protozoan beta-carbonic anhydrase from Trichomonas vaginalis. J Enzyme Inhib Med Chem 2020, 35 (1), 1292–1299. [PubMed: 32515610]

(19). Urbanski LJ; Angeli A; Hytonen VP; Di Fiore A; Parkkila S; De Simone G; Supuran CT Inhibition of the newly discovered betacarbonic anhydrase from the protozoan pathogen Trichomonas vaginalis with inorganic anions and small molecules. J Inorg Biochem 2020, 213, 111274. [PubMed: 33068968]

(20). Hopper M; Yun JF; Zhou B; Le C; Kehoe K; Le R; Hill R; Jongeward G; Debnath A; Zhang L; Miyamoto Y; Eckmann L; Land KM; Wrischnik LA Auranofin inactivates Trichomonas vaginalis thioredoxin reductase and is effective against trichomonads in vitro and in vivo. Int J Antimicrob Agents 2016, 48 (6), 690–694. [PubMed: 27839893]

(21). Debnath A; Parsonage D; Andrade RM; He C; Cobo ER; Hirata K; Chen S; Garcia-Rivera G; Orozco E; Martinez MB; Gunatilleke SS; Barrios AM; Arkin MR; Poole LB; McKerrow JH; Reed SL A high-throughput drug screen for Entamoeba histolytica identifies a new lead and target. Nat Med 2012, 18 (6), 956–960. [PubMed: 22610278]

(22). Navarro M Gold complexes as potential anti-parasitic agents. Coordin Chem Rev 2009, 253 (11–12), 1619–1626.

(23). Kean WF; Kean IR Clinical pharmacology of gold. Inflammopharmacology 2008, 16 (3), 112–125. [PubMed: 18523733]

(24). Leitsch D; Muller J; Muller N Evaluation of Giardia lamblia thioredoxin reductase as drug activating enzyme and as drug target. Int J Parasitol Drugs Drug Resist 2016, 6 (3), 148–153. [PubMed: 27485086]

(25). Kuntz AN; Davioud-Charvet E; Sayed AA; Califf LL; Dessolin J; Arner ES; Williams DL Thioredoxin glutathione reductase from Schistosoma mansoni: an essential parasite enzyme and a key drug target. PLoS Med 2007, 4 (6), e206. [PubMed: 17579510]

(26). Zhang C; Bourgeade Delmas S; Fernandez Alvarez A; Valentin A; Hemmert C; Gornitzka H Synthesis, characterization, and antileishmanial activity of neutral N-heterocyclic carbenes gold(I) complexes. Eur J Med Chem 2018, 143, 1635–1643. [PubMed: 29133045]

(27). Koko WS; Jentzsch J; Kalie H; Schobert R; Ersfeld K; Al Nasr IS; Khan TA; Biersack B Evaluation of the antiparasitic activities of imidazol-2-ylidene-gold(I) complexes. Arch Pharm (Weinheim) 2020, 353 (5), e1900363. [PubMed: 32149417]

(28). Winter I; Lockhauserbaumer J; Lallinger-Kube G; Schobert R; Ersfeld K; Biersack B Anti-trypanosomal activity of cationic N-heterocyclic carbene gold(I) complexes. Mol Biochem Parasitol 2017, 214, 112–120. [PubMed: 28522152]

(29). Wu B; Yang X; Yan M Synthesis and structure-activity relationship study of antimicrobial auranofin against ESKAPE pathogens. J Med Chem 2019, 62 (17), 7751–7768. [PubMed: 31386365]

(30). Parsonage D; Sheng F; Hirata K; Debnath A; McKerrow JH; Reed SL; Abagyan R; Poole LB; Podust LM X-ray structures of thioredoxin and thioredoxin reductase from Entamoeba histolytica and prevailing hypothesis of the mechanism of Auranofin action. J Struct Biol 2016, 194 (2), 180–190. [PubMed: 26876147]

(31). Mentel M; Zimorski V; Haferkamp P; Martin W; Henze K Protein import into hydrogenosomes of Trichomonas vaginalis involves both N-terminal and internal targeting signals: a case study of thioredoxin reductases. Eukaryot Cell 2008, 7 (10), 1750–1757. [PubMed: 18676956]

(32). Schlosser S; Leitsch D; Duchene M Entamoeba histolytica: identification of thioredoxin-targeted proteins and analysis of serine acetyltransferase-1 as a prototype example. Biochem J 2013, 451 (2), 277–288. [PubMed: 23398389]

(33). Williams CF; Lloyd D; Kolarich D; Alagesan K; Duchene M; Cable J; Williams D; Leitsch D Disrupted intracellular redox balance of the diplomonad fish parasite Spironucleus vortens by 5-nitroimidazoles and garlic-derived compounds. Vet Parasitol 2012, 190 (1–2), 62–73. [PubMed: 22677132]

(34). Leitsch D; Burgess AG; Dunn LA; Krauer KG; Tan K; Duchene M; Upcroft P; Eckmann L; Upcroft JA Pyruvate:ferredoxin oxidoreductase and thioredoxin reductase are involved in 5-nitroimidazole activation while flavin metabolism is linked to 5-nitroimidazole resistance in Giardia lamblia. J Antimicrob Chemother 2011, 66 (8), 1756–1765. [PubMed: 21602576]

(35). Dunne RL; Dunn LA; Upcroft P; O'Donoghue PJ; Upcroft JA Drug resistance in the sexually transmitted protozoan Trichomonas vaginalis. Cell Res 2003, 13 (4), 239–249. [PubMed: 12974614]

(36). Wright JM; Dunn LA; Kazimierczuk Z; Burgess AG; Krauer KG; Upcroft P; Upcroft JA Susceptibility in vitro of clinically metronidazole-resistant Trichomonas vaginalis to nitazoxanide, toyocamycin, and 2-fluoro-2'-deoxyadenosine. Parasitol Res 2010, 107 (4), 847–853. [PubMed: 20532912]

(37). Bradic M; Warring SD; Tooley GE; Scheid P; Secor WE; Land KM; Huang PJ; Chen TW; Lee CC; Tang P; Sullivan SA; Carlton JM Genetic indicators of drug resistance in the highly repetitive genome of Trichomonas vaginalis. Genome Biol Evol 2017, 9 (6), 1658–1672. [PubMed: 28633446]

(38). Cobo ER; Eckmann L; Corbeil LB Murine models of vaginal trichomonad infections. Am J Trop Med Hyg 2011, 85 (4), 667–673. [PubMed: 21976570]

(39). Tejman-Yarden N; Miyamoto Y; Leitsch D; Santini J; Debnath A; Gut J; McKerrow JH; Reed SL; Eckmann L A reprofiled drug, auranofin, is effective against metronidazole-resistant Giardia lamblia. Antimicrob Agents Chemother 2013, 57 (5), 2029–2035. [PubMed: 23403423]

(40). Madeira JM; Gibson DL; Kean WF; Klegeris A The biological activity of auranofin: implications for novel treatment of diseases. Inflammopharmacology 2012, 20 (6), 297–306. [PubMed: 22965242]

(41). Isakov E; Weisman-Shomer P; Benhar M Suppression of the pro-inflammatory NLRP3/interleukin-1beta pathway in macrophages by the thioredoxin reductase inhibitor auranofin. Biochim Biophys Acta 2014, 1840 (10), 3153–3161. [PubMed: 25065288]

(42). Hwangbo H; Kim SY; Lee H; Park SH; Hong SH; Park C; Kim GY; Leem SH; Hyun JW; Cheong J; Choi YH Auranofin enhances sulforaphane-mediated apoptosis in hepatocellular carcinoma Hep3B cells through inactivation of the PI3K/Akt signaling pathway. Biomol Ther (Seoul) 2020, 28 (5), 443–455. [PubMed: 32856616]

(43). Saei AA; Gullberg H; Sabatier P; Beusch CM; Johansson K; Lundgren B; Arvidsson PI; Arner ESJ; Zubarev RA Comprehensive chemical proteomics for target deconvolution of the redox active drug auranofin. Redox Biol 2020, 32, 101491. [PubMed: 32199331]

(44). Abhishek S; Sivadas S; Satish M; Deeksha W; Rajakumara E Dynamic basis for auranofin drug recognition by thiol-reductases of human pathogens and intermediate coordinated adduct formation with catalytic cysteine residues. ACS Omega 2019, 4 (5), 9593–9602. [PubMed: 31460050]

(45). Talib J; Beck JL; Ralph SF A mass spectrometric investigation of the binding of gold antiarthritic agents and the metabolite [Au(CN)2]- to human serum albumin. J Biol Inorg Chem 2006, 11 (5), 559–570. [PubMed: 16791640]

(46). Leitsch D; Williams CF; Hrdy I Redox pathways as drug targets in microaerophilic parasites. Trends Parasitol 2018, 34 (7), 576–589. [PubMed: 29807758]

(47). Andrade RM; Reed SL New drug target in protozoan parasites: the role of thioredoxin reductase. Front Microbiol 2015, 6, 975. [PubMed: 26483758]

(48). Froscio M; Murray AW; Hurst NP Inhibition of protein kinase C activity by the antirheumatic drug auranofin. Biochem Pharmacol 1989, 38 (13), 2087–2089. [PubMed: 2735946]

(49). Krishnamurthy D; Karver MR; Fiorillo E; Orru V; Stanford SM; Bottini N; Barrios AM Gold(I)-mediated inhibition of protein tyrosine phosphatases: a detailed in vitro and cellular study. J Med Chem 2008, 51 (15), 4790–4795. [PubMed: 18605719]

(50). Tian S; Siu FM; Lok CN; Fung YME; Che CM Anticancer auranofin engages 3-hydroxy-3-methylglutaryl-coenzyme A reductase (HMGCR) as a target. Metallomics 2019, 11 (11), 1925–1936. [PubMed: 31631207]

(51). Carlton JM; Hirt RP; Silva JC; Delcher AL; Schatz M; Zhao Q; Wortman JR; Bidwell SL; Alsmark UC; Besteiro S; Sicheritz-Ponten T; Noel CJ; Dacks JB; Foster PG; Simillion C; Van de Peer Y; Miranda-Saavedra D; Barton GJ; Westrop GD; Muller S; Dessi D; Fiori PL; Ren Q; Paulsen I; Zhang H; Bastida-Corcuera FD; Simoes-Barbosa A; Brown MT; Hayes RD; Mukherjee M; Okumura CY; Schneider R; Smith AJ; Vanacova S; Villalvazo M; Haas BJ; Pertea M; Feldblyum TV; Utterback TR; Shu CL; Osoegawa K; de Jong PJ; Hrdy I; Horvathova L; Zubacova Z; Dolezal P; Malik SB; Logsdon JM Jr.; Henze K; Gupta A; Wang CC; Dunne RL; Upcroft JA; Upcroft P; White O; Salzberg SL; Tang P; Chiu CH; Lee YS; Embley TM; Coombs GH; Mottram JC; Tachezy J; Fraser-Liggett CM; Johnson PJ Draft genome sequence of the sexually transmitted pathogen Trichomonas vaginalis. Science 2007, 315 (5809), 207–212. [PubMed: 17218520]

(52). Marzo T; Cirri D; Gabbiani C; Gamberi T; Magherini F; Pratesi A; Guerri A; Biver T; Binacchi F; Stefanini M; Arcangeli A; Messori L Auranofin, Et3PAuCl, and Et3PAuI are highly cytotoxic on colorectal cancer cells: A chemical and biological study. ACS Med Chem Lett 2017, 8 (10), 997–1001. [PubMed: 29057040]

(53). duBouchet L; McGregor JA; Ismail M; McCormack WM A pilot study of metronidazole vaginal gel versus oral metronidazole for the treatment of Trichomonas vaginalis vaginitis. Sex Transm Dis 1998, 25 (3), 176–179. [PubMed: 9524997]

(54). Schwebke JR; Lensing SY; Sobel J Intravaginal metronidazole/miconazole for the treatment of vaginal trichomoniasis. Sex Transm Dis 2013, 40 (9), 710–714. [PubMed: 23949586]

(55). Lushbaugh WB; Blossom AC; Shah PH; Banga AK; Jaynes JM; Cleary JD; Finley RW Use of intravaginal microbicides to prevent acquisition of Trichomonas vaginalis infection in Lactobacillus-pretreated, estrogenized young mice. Am J Trop Med Hyg 2000, 63 (5–6), 284–289. [PubMed: 11421379]

(56). Zhang Y; Miyamoto Y; Ihara S; Yang JZ; Zuill DE; Angsantikul P; Zhang Q; Gao W; Zhang L; Eckmann L Composite thermoresponsive hydrogel with auranofin-loaded nanoparticles for topical treatment of vaginal trichomonad infection. Adv Ther (Weinh) 2019, 2 (12), 1900157. [PubMed: 32377561]

(57). Cunningham FE; Kraus DM; Brubaker L; Fischer JH Pharmacokinetics of intravaginal metronidazole gel. J Clin Pharmacol 1994, 34 (11), 1060–1065. [PubMed: 7876396]

(58). Pearson S; Scarano W; Stenzel MH Micelles based on gold-glycopolymer complexes as new chemotherapy drug delivery agents. Chem Commun (Camb) 2012, 48 (39), 4695–4697. [PubMed: 22473015]

(59). McGusty E; Sutton B Phosphine or phosphite gold complexes of thiomalic acid. U.S. Patent US3718679A, Apr 27, 1971.

(60). Rubbiani R; Can S; Kitanovic I; Alborzinia H; Stefanopoulou M; Kokoschka M; Monchgesang S; Sheldrick WS; Wolfl S; Ott I Comparative in vitro evaluation of N-heterocyclic carbene gold(I) complexes of the benzimidazolylidene type. J Med Chem 2011, 54 (24), 8646–8657. [PubMed: 22039997]

(61). Electri MM; Scovell WM Synthesis and spectroscopic characterization of (Triethylphosphine)gold(I) complexes Aux(Pet3) (X=Cl, Br, Cn, Scn), [Aul(Pet3)+] (L=Sme2, Sc(Nh2)2, H2o), and (Mu-S)[Au(Pet3)]2. Inorg Chem 1990, 29 (3), 480–484.

(62). Carrasco D; Garcia-Melchor M; Casares JA; Espinet P Dramatic mechanistic switch in Sn/Au(I) group exchanges: transmetalation vs. oxidative addition. Chem Commun (Camb) 2016, 52 (23), 4305–4308. [PubMed: 26960420]

(63). Brown DM; Upcroft JA; Dodd HN; Chen N; Upcroft P Alternative 2-keto acid oxidoreductase activities in Trichomonas vaginalis. Mol Biochem Parasitol 1999, 98 (2), 203–214. [PubMed: 10080389]

(64). Goldman LM; Upcroft JA; Workowski K; Rapkin A Treatment of metronidazole-resistant Trichomonas vaginalis. Sex Health 2009, 6 (4), 345–347. [PubMed: 19917205]

(65). Clark CG; Diamond LS Methods for cultivation of luminal parasitic protists of clinical importance. Clin Microbiol Rev 2002, 15 (3), 329–341. [PubMed: 12097242]

(66). Miyamoto Y; Kalisiak J; Korthals K; Lauwaet T; Cheung DY; Lozano R; Cobo ER; Upcroft P; Upcroft JA; Berg DE; Gillin FD; Fokin VV; Sharpless KB; Eckmann L Expanded therapeutic potential in activity space of next-generation 5-nitroimidazole antimicrobials with broad structural diversity. Proc Natl Acad Sci U S A 2013, 110 (43), 17564–17569. [PubMed: 24101497]

(67). Thompson JD; Gibson TJ; Plewniak F; Jeanmougin F; Higgins DG The CLUSTAL_X windows interface: flexible strategies for multiple sequence alignment aided by quality analysis tools. Nucleic Acids Res 1997, 25 (24), 4876–4882. [PubMed: 9396791]

(68). Kumar S; Stecher G; Li M; Knyaz C; Tamura K MEGA X: Molecular evolutionary genetics analysis across computing platforms. Mol Biol Evol 2018, 35 (6), 1547–1549. [PubMed: 29722887]

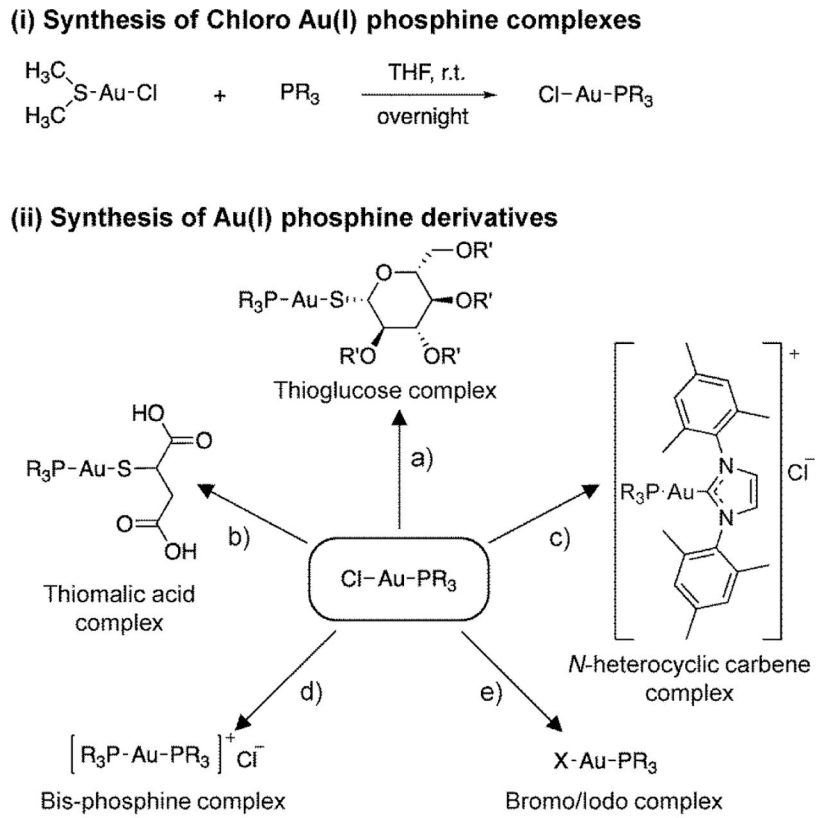

Figure 1. Synthetic scheme for gold(I) complexes.

General scheme employed in the synthesis of gold(I) complexes involved two steps: (i) synthesis of Cl-Au-PR_3 complexes from (dimethylsulfide)gold(I) chloride and the corresponding PR_3, and (ii) replacement of Cl with various thiols, other halides, or PR"$_3$ ligands.

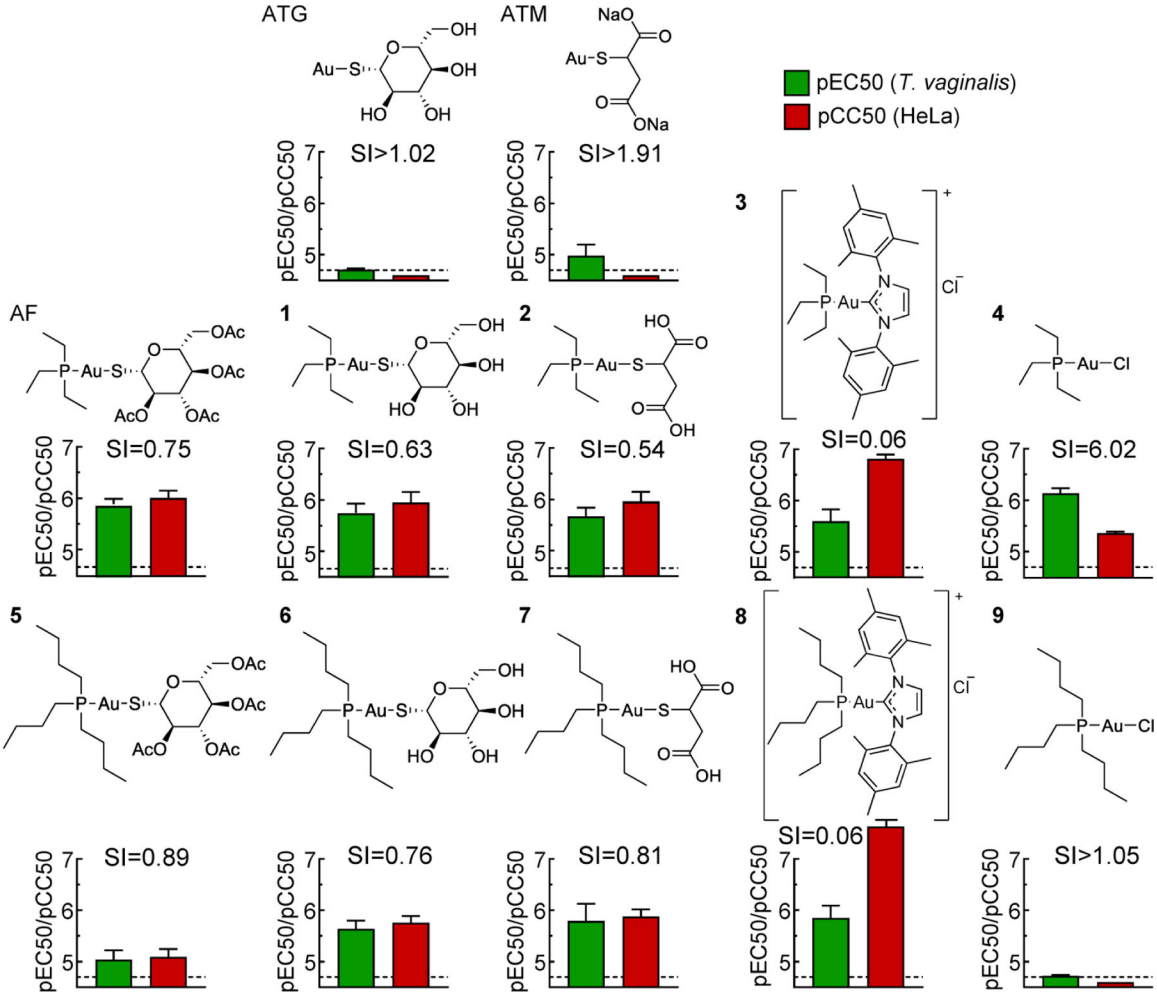

Figure 2. Trichomonacidal activity and human cytotoxicity of FDA-approved and related gold(I) complexes.

The activity of the indicated gold(I) complexes against *T. vaginalis* F1623 (pEC50, green bars) and human Hela cells (pCC50, red bars) were determined in 24–48 h growth and survival assays. Results are shown as mean + SEM (n≥3 independent experiments). Selectivity index (SI) was calculated as CC50/EC50. The dashed line depicts the assay sensitivity.

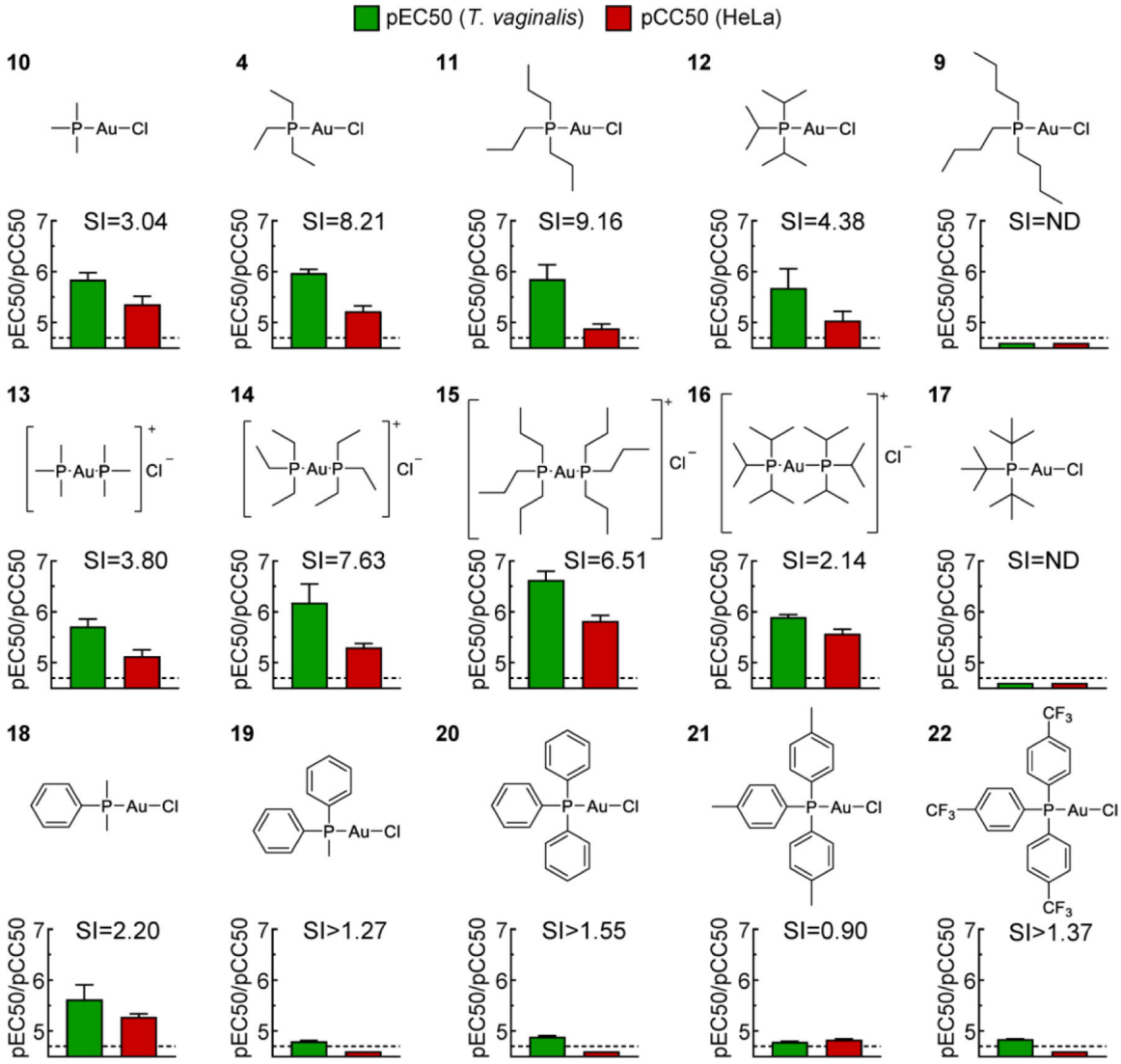

Figure 3. Trichomonacidal activity and human cytotoxicity of gold(I) phosphine derivatives.

The activity of the depicted gold(I) complexes against *T. vaginalis* F1623 (pEC50, green bars) and human Hela cells (pCC50, red bars) were determined in 24–48 h growth and survival assays. Results are shown as mean + SEM (n≥3 independent experiments). Two of the compounds (**4** and **9**) were also tested in experiments in Fig. 2, but the data in this figure were derived independently as controls along with the other depicted compounds. Selectivity index (SI) was calculated as CC50/EC50. The dashed line shows the assay sensitivity.

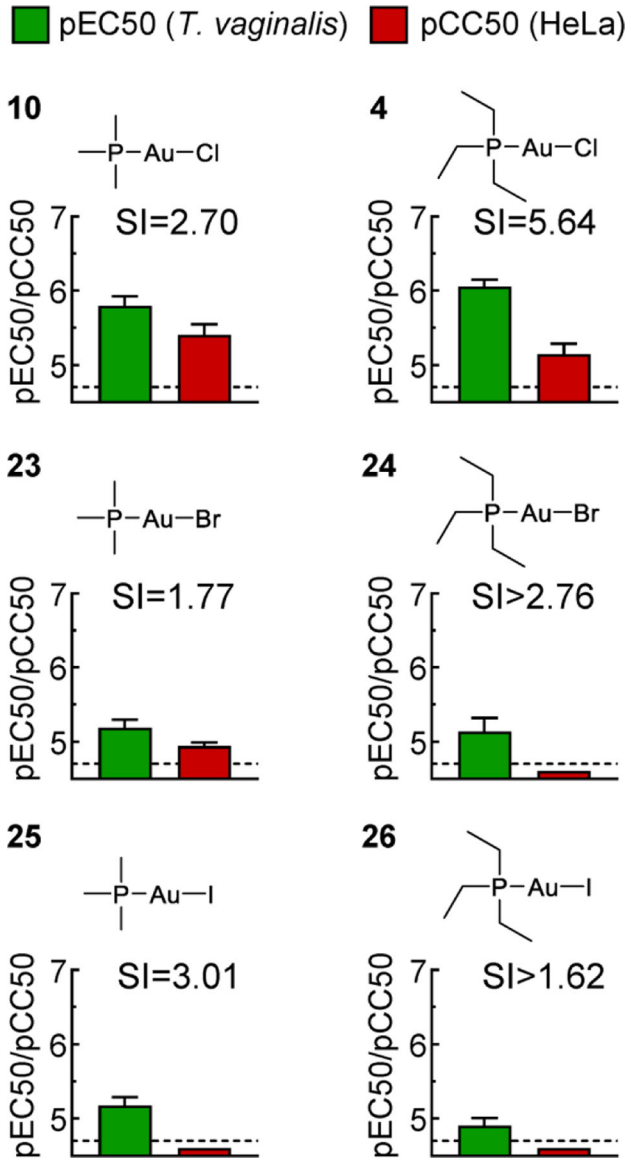

Figure 4. Activity of gold(I) phosphine halides against *T. vaginalis* and human cells.

The activity of the depicted gold(I) complexes against *T. vaginalis* F1623 (pEC50, green bars) and human Hela cells (pCC50, red bars) were determined in 24–48 h growth and survival assays. Results are shown as mean + SEM (n≥3 independent experiments). Two of the compounds (**4** and **10**) were also tested in experiments in Fig. 3, but the data in this figure were derived independently as controls along with the other depicted compounds. Selectivity index (SI) was calculated as CC50/EC50. The dashed line shows the assay sensitivity.

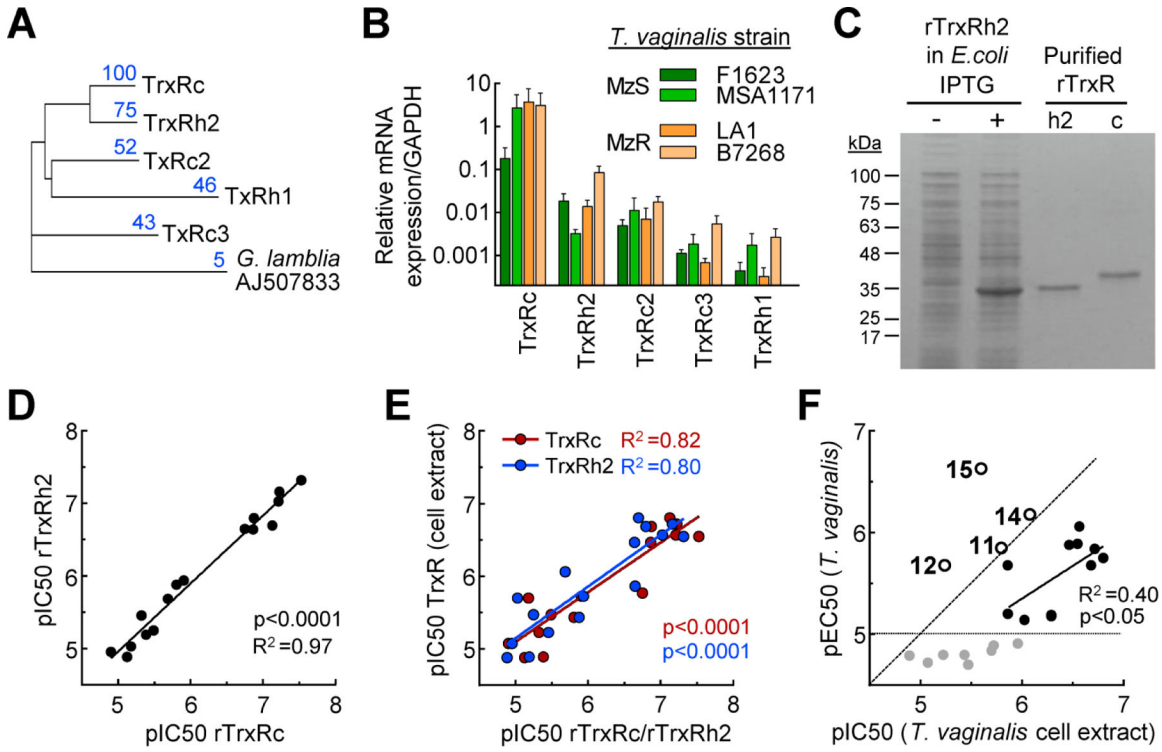

Fig. 5. *T. vaginalis* TrxR isoform expression and inhibition by gold(I) complexes.

A. Dendrogram of amino acid sequence alignments of the five *T. vaginalis* TrxR isoforms, with TrxR of *G. lamblia* as a root. Blue numbers refer to percentage amino acid identity of the respective isoform relative to TrxRc (100%). **B.** Expression levels of the five TrxR isoforms were analyzed by qPCR in two metronidazole-sensitive (MzS) lines of *T. vaginalis* (green bars) and two metronidazole-resistant (MzR) lines (orange bars). TrxR levels are expressed relative to GAPDH and represent mean + SEM of four independent experiments. **C.** Coomassie Blue-stained SDS-PAGE gel of *E. coli* BL21extracts before (−) and after (+) IPTG induction of recombinant TrxRh2, and after Ni-NTA affinity purification of this TrxR isoform (h2) and purified recombinant rTrxRc (c). **D.** *In vitro* inhibitory activities (pIC50) of a library of gold(I) complexes against the two indicated recombinant TrxR isoforms. **E.** Correlation of *in vitro* inhibitory activity (pIC50) of gold(I) complexes against the two most abundant recombinant TrxR isoforms (red, TrxRc; blue, TrxRh2) and total TrxR in whole-cell extracts of *T.vaginalis* F1623. **F.** Correlation of TrxR inhibition (pIC50) in whole-cell extracts and trichomonacidal activity (pEC50) of gold(I) complexes. In panels D-F, each dot represents one gold(I) complex (mean, n=3 experiments). Pearson correlation coefficients (R^2) and their significances (p value) were calculated, and regression lines are shown. In F, correlation was only calculated for the compounds with good trichomonacidal activity (pEC50>5) and a pEC50/pIC50 ratio of ≤1 (black dots), while compounds with low trichomonacidal activity (gray dots below gray line) and compounds with pEC50/pIC50 ratios >1 (circled dots with compound names) were not considered for this purpose. The latter are likely to act by mechanisms other than TrxR inhibition. The diagonal dashed line in F represents a unit slope with pEC50:pIC50 ratios of one.

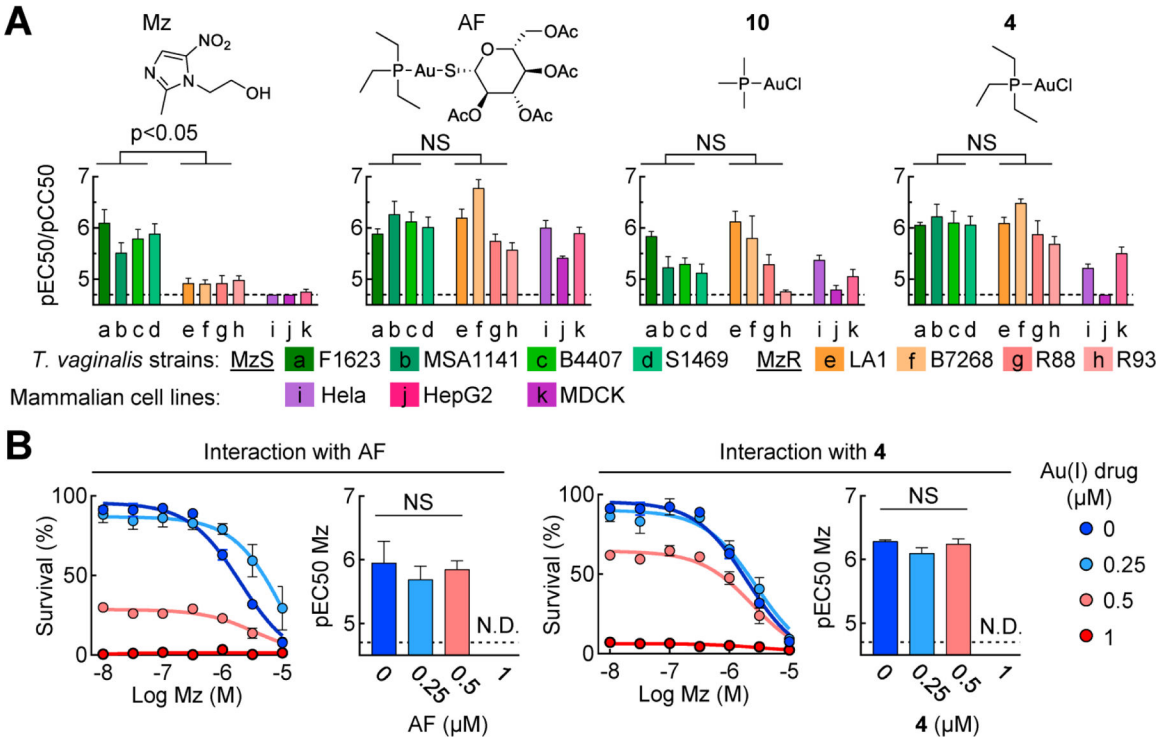

Fig. 6. Gold(I) complexes overcome resistance of *T. vaginalis* to metronidazole.

A. The depicted gold(I) complexes, and metronidazole (Mz) as a control, were tested for activity (pEC50) against the eight listed *T. vaginalis* strains, four of which were Mz-sensitive (MzS; strains a-d, green bars) and four were Mz-resistant (MzR; strains e-h, orange/pink bars). Gold(I) complexes were also evaluated for cytotoxicity (pCC50; purple//red bars) using the indicated transformed (HeLa, HepG) and non-transformed (MDCK) mammalian cell lines. Results are given as mean + SEM (n≥3 independent experiments). Significance between the MzS and MzR groups was determined by unpaired t-test. **B.** Synergy in trichomonacidal activity of two gold(I) complexes and Mz was determined in a 24 h growth and survival assay. The graphs on the left show % cell survival relative to untreated cells at different Mz concentrations for each of four depicted gold(I) drug concentrations (means ± SEM, n≥3 experiments). The bar graphs on the right show the calculated pEC50 values for Mz in the presence of the indicated gold(I) drug concentrations. Significance between the groups was determined by one-way ANOVA (NS, not significant; ND, not determined). Dashed lines depict assay sensitivity.

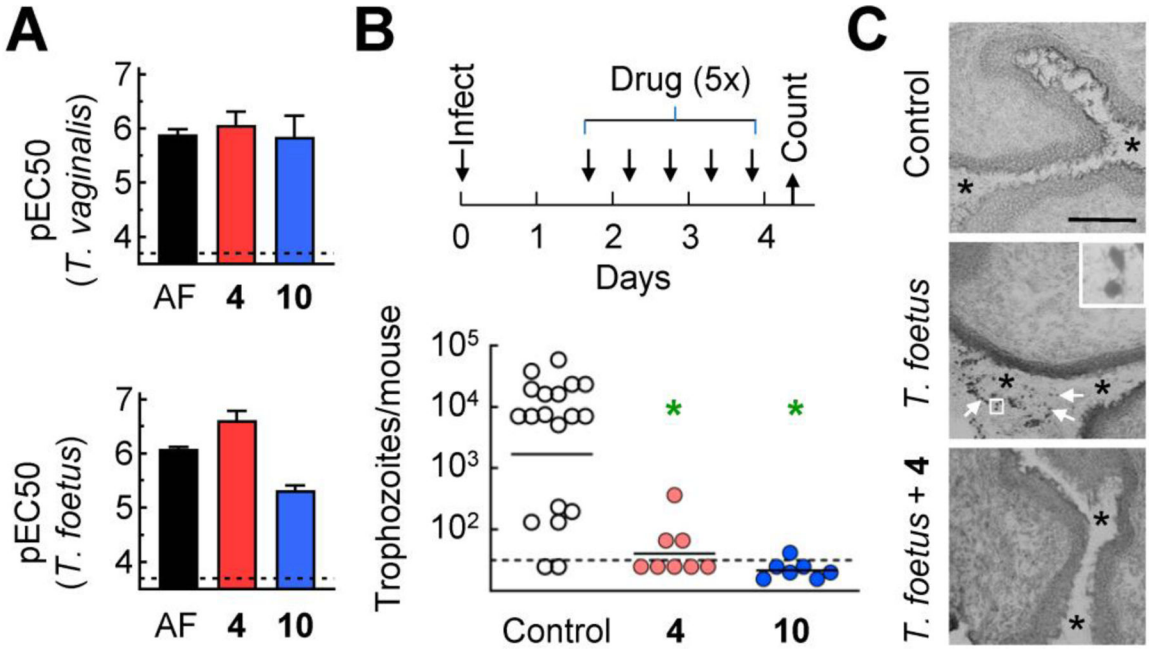

Fig. 7. ***In vivo*** **efficacy of gold(I) complex against vaginal trichomonad infection.**

A. The indicated gold(I) complexes were tested for activity (pEC50) against *T. vaginalis* F1623 (top panel) and *T. foetus* (bottom panel). Data are shown as mean + SEM (n≥3 experiments). **B.** Weanling female BALB/cJ mice were infected intravaginally with *T. foetus* trophozoites and after one day, mice were treated intravaginally with gold(I) complexes or vehicles (Control) as indicated in the timeline. On day 4, live trophozoites were enumerated in vaginal washes. Each point represents an individual mouse, horizontal bars show geometric means (*P<0.05 relative to controls, Kruskal-Wallis test). Dashed lines show the detection limit of the assays in both panels. **C.** Frozen sections of the vaginal tract were prepared and stained with Wright-Giemsa stain. Top panel, non-infected controls; middle panel, *T. foetus* infected, no treatment (4 days after infection; arrows depict individual trophozoites, insert shows boxed area at higher magnification); bottom panel: *T. foetus* infected, treated with compound **4** as outlined in panel B (4 days after infection). Asterisks in all three panels highlight the vaginal lumen. Size bar in top panel represents 50 μm.